HHS Public Access

Author manuscript

Neurobiol Dis. Author manuscript; available in PMC 2025 December 01.

Published in final edited form as:

Neurobiol Dis. 2025 November ; 216: 107128. doi:10.1016/j.nbd.2025.107128.

Single nucleus RNA sequencing unveils relationship between microglia and endothelial cells in mixed Alzheimer's disease and vascular pathology

Oluwatosin A. Olayinka[a,b], **Nicholas O'Neill**[a,b], **Jenny A. Empawi**[b], **Payton Bock**[a], **Junming Hu**[a,b], **Hannah Rickner**[c], **Melissa Wong**[c], **Thor D. Stein**[d,g,h], **Benjamin Wolozin**[c,e], **Lindsay A. Farrer**[a,b,e,f,i,j,*], **Xiaoling Zhang**[a,b,i,**]

[a]Bioinformatics Program, Boston University, 24 Cummington Mall, Boston, MA 02215, USA

[b]Departments of Medicine (Biomedical Genetics), 72 East Concord St., Boston, MA 02118, USA

[c]Anatomy & Neurobiology, 72 East Concord St., Boston, MA 02118, USA

[d]Pathology and Laboratory Medicine, USA

[e]Neurology, 72 East Concord St., Boston, MA 02118, USA

[f]Ophthalmology, Boston University Chobanian & Avedisian School of Medicine, 72 East Concord St., Boston, MA 02118, USA

[g]VA Boston Healthcare System, 150 S Huntington Ave, Boston, MA 02130, USA

[h]VA Bedford Healthcare System, 200 Springs Rd, Bedford, MA 01730, USA

[i]Department of Biostatistics, Boston University School of Public Health, 715 Albany St., Boston, MA 02118, USA

[j]Department of Epidemiology, Boston University School of Public Health, 715 Albany St., Boston, MA 02118, USA

Abstract

Single-nucleus RNA sequencing (snRNAseq) allows for the dissection of cell type-specific transcriptional profiles. We evaluated differential gene expression using snRNAseq data generated

*Correspondence to: LA. Farrer, Boston University School of Medicine, Biomedical Genetics E200, 72 East Concord Street, Boston, MA 02118, USA. farrer@bu.edu (L.A. Farrer). **Correspondence to: X Zhang, Boston University School of Medicine, Biomedical Genetics E223, 72 East Concord Street, Boston, MA 02118, USA. zhangxl@bu.edu (X. Zhang).

CRediT authorship contribution statement

Oluwatosin A. Olayinka: Writing – review & editing, Writing – original draft, Methodology, Investigation, Formal analysis, Conceptualization. **Nicholas O'Neill:** Writing – review & editing, Software. **Jenny A. Empawi:** Writing – review & editing, Formal analysis. **Payton Bock:** Writing – review & editing, Formal analysis. **Junming Hu:** Writing – review & editing, Formal analysis. **Hannah Rickner:** Writing – review & editing, Investigation. **Melissa Wong:** Writing – review & editing, Investigation. **Thor D. Stein:** Writing – review & editing, Methodology. **Benjamin Wolozin:** Writing – review & editing, Supervision, Resources, Methodology. **Lindsay A. Farrer:** Writing – review & editing, Supervision, Resources, Project administration, Funding acquisition, Conceptualization. **Xiaoling Zhang:** Writing – review & editing, Supervision, Methodology.

Declaration of competing interest

The authors declare that they have no known competing financial interests or personal relationships that could have appeared to influence the work reported in this paper.

from hippocampal region tissue donated by 11 Boston University Alzheimer's Disease Research Center (BU-ADRC) participants with neuropathologically confirmed Alzheimer's disease (AD) with or without co-existing pathology (AD only = 3, AD+vascular disease (Vas) = 6, AD+Lewy body disease (LBD) = 2). Expression of 19,893 genes was compared between AD+Vas and other AD groups for each cell type. Co-expression modules were identified in a set of 174 bulk RNAseq hippocampal samples from BU-ADRC. Modules enriched in differentially expressed genes (DEGs) were identified using Fisher's exact tests. The overlap between DEGs and co-expression modules was incorporated into quantitative gene set analysis. AD+Vas subjects showed decreased expression of genes related to immune activation in microglia ($t = -2.67$, $p = 2.72 \times 10^{-2}$). Expression of these genes was negatively associated with expression of receptors *P2RY12* and *CX3CR1* ($r = -0.87$, $p = 1.70 \times 10^{-2}$), which have been linked to microglial migration and activation, respectively. Expression of genes that negatively regulate angiogenesis in endothelial cells was decreased ($t = -4.84$, $p = 1.49 \times 10^{-3}$) and associated with expression of the microglial activation genes in the BU-ADRC dataset ($r = 0.68$, $p = 1.63 \times 10^{-2}$). This association and the finding of upregulation of *P2RY12* in AD+Vas samples were replicated in 393 ROSMAP Study dorsolateral prefrontal cortex snRNAseq samples ($r = 0.34$, $p = 8.37 \times 10^{-12}$ and z = 5.82, $p_{FDR} = 8.73 \times 10^{-6}$, respectively). In summary, we found an expression profile in brain tissue from individuals with AD+Vas pathology that is associated with reduced activation and increased migration in microglia and angiogenesis in endothelial cells.

Keywords

Single-nucleus RNA sequencing; Alzheimer's disease; Lewy body disease; Vascular disease; Microglia; Endothelial cells

1. Introduction

Alzheimer's disease (AD) is a neurodegenerative disorder and the leading cause of dementia. It is characterized by the presence of neurofibrillary tangles and amyloid plaques in the brain, progressive cognitive impairment, and memory loss (Kumar et al., 2023). Increasingly more attention has been given to mixed-pathology AD (MxAD) where hallmark AD proteins (i.e., amyloid-β and hyperphosphorylated tau) co-occur with pathological markers of other diseases. Observational studies have found a high prevalence of MxAD in AD patients, with one study showing 91 % of AD patients having additional neuropathology (Boyle et al., 2018). Among the most common co-occurring pathologies with AD include vascular disease (Vas) and Lewy body disease (LBD), with these respectively occurring in approximately 71 % and 15 % of those with AD pathology (Boyle et al., 2018). Therefore, a better understanding of how these combined pathologies affect the pathogenesis and progression of the disease may provide valuable insights into more effective treatment and potential new therapeutic targets. This is especially important for the highly prevalent combined AD and vascular pathology. Cerebrovascular lesions associated with cognitive decline encompass a spectrum of subtypes, including large artery atherosclerosis, cerebral small vessel disease (e.g., arteriolosclerosis), cortical and subcortical infarcts, and hypoperfusive injuries following systemic events such as cardiac

arrest. These vascular pathologies often overlap with AD-related changes, potentially accelerating neurodegeneration and influencing clinical presentation.

Cardiovascular risk factors, in particular, have been linked to worsened AD-related outcomes. For instance, in an observational cohort study, a mid-life cardiovascular risk factor related to hypertension, body mass index, diabetes, and blood lipid levels was strongly associated with greater amyloid deposition in the brain (Gottesman et al., 2017). Other studies have also found that similar scores are positively associated with AD and non-AD forms of dementia as well as cerebral infarctions and atherosclerosis later in life (Song et al., 2021). This link is further supported by the genetic association between ischemic stroke risk and AD and all-cause dementia, respectively (Luo et al., 2025). Genetic associations between AD and plasma lipid traits also support this relationship (Broce et al., 2019). This all suggests that vascular dysfunction may play a role in exacerbating AD, highlighting the need to study the co-occurrence of Vas with AD.

Both genome-wide association (Bellenguez et al., 2022; Jansen et al., 2019; Kunkle et al., 2019; Wightman et al., 2021) (GWAS) and molecular biology studies have implicated glial cell types in AD pathology (Dzamba et al., 2016; Kim et al., 2018; Nordengen et al., 2019; Uddin and Lim, 2022). For instance, many genes implicated in AD through GWAS are highly or exclusively expressed in specific glial cells. Variants in the *APOE*, *TREM2*, *CR1*, and *MS4A* genes have been consistently associated with AD and are highly expressed in microglia (Hansen et al., 2018). Furthermore, the presence and expression of many of these genes have been linked to microglial function in AD mouse models (Crehan et al., 2013; Lee et al., 2023; Song et al., 2018). These studies highlight potential roles particular cell types may play in AD biology.

Single-nucleus RNA sequencing (snRNAseq) allows for quantitative measurement of gene expression at the cellular level (Grindberg et al., 2013; Wu et al., 2019) and has been conducted in tissue from a wide variety of human brain regions (Grubman et al., 2019; Lau et al., 2020; Mathys et al., 2019; Morabito et al., 2021; Olah et al., 2020; Zhou et al., 2020), revealing novel information about cell-specific processes involved in AD. Although single-cell sequencing has several advantages over snRNAseq, including capturing cytoplasmic transcripts, snRNAseq is a more appropriate technology to capture cell-level expression in the central nervous system because it doesn’t require dissociating neural and glial cells (Ding et al., 2020). With large frozen brain samples, snRNAseq also allows for unraveling gene expression information at a sub-cell-type level, including subtypes of microglia. For example, Haney et al. found an elevated proportion of lipid droplet-accumulating microglia (LDAM), a subtype distinct from the typical homeostatic microglia (HOM), in AD cases compared to controls (Haney et al., 2024). snRNAseq studies have also revealed unique expression changes in brain endothelial cells from individuals with Lewy body disease (Feleke et al., 2021) and vascular dementia (Mitroi et al., 2022). However, to date, few snRNAseq studies have been performed using tissue from the hippocampal region, with those studies that do exist not focusing on MxAD specifically (Mathys et al., 2024; Yang et al., 2022). The accumulation of amyloid plaques and neurofibrillary tangles often concentrates in the hippocampus and spreads to other parts of the brain (Toda et al., 2019). Thus, the development of biomarkers based on measurable changes in the hippocampal

region may potentiate early detection and diagnosis. Early intervention and targeted treatments might mitigate the effects of neurodegeneration. Furthermore, identification of molecular and cellular changes in the hippocampus could increase understanding of the underlying causes of dementia and steps involved in the disease progression and thereby lead to the development of more effective therapies.

In this study, we sought to identify cell type-level molecular characteristics that distinguish samples with combined AD and Vas pathologies (AD+Vas) from those with exclusive AD pathology (AD only) or combined AD and LBD pathologies (AD+LBD). Because AD+LBD is much less common than those with AD alone or AD+Vas, and given that our primary focus is to examine single-cell transcriptional changes associated with vascular pathology in the context of AD, we combined the AD-only and AD+LBD samples into a vascular-pathology–negative AD group for comparison with AD+Vas samples.

2. Results

2.1. Differential gene expression across cell types

A total of 80,105 nuclei distributed among 14 different cell types remain for analysis after quality control filtering (Fig. 1a). The relatively large number of nuclei enabled the identification of distinct cellular subtypes, including arterial, capillary, and venous endothelial cells (Supplemental Fig. 1) as well as LDAM and HOM (Supplemental Fig. 2), which were classified in accordance with another recent snRNAseq study (Haney et al., 2024). Approximately 76 % of the significant DEGs ($|logFC| > 0.15$, $p_{bonferroni} < 10^{-6}$) identified in the AD+Vas group were downregulated, suggesting a general pattern of transcriptional downregulation in brains with AD+Vas pathology. This pattern was evident in astrocytes and oligodendrocyte progenitor cells, and especially in microglia and endothelial cells. For example, only 18 of 263 DEGs in microglia and only one of 370 in endothelial cells were upregulated (Fig. 1c). These cell-type-specific changes account for almost half (43.7 %) of all unique DEGs in the AD+Vas group. Furthermore, many DEGs were observed in microglia and endothelial cells despite their relatively low cell proportions (Fig. 1b).

Differential gene expression analysis across cell types also revealed the unique regulation of transcriptional programs in each cell type evidenced by the very small proportion of cross-cellular sharing of DEGs (Fig. 1d). Supporting this finding, the enrichment of WGCNA modules in DEGs is highly cell-type dependent (Fig. 2a, Table 1). For example, the *M2* module is associated with innate immune response and is enriched in the microglial downregulated DEGs (OR = 5.99, $p_{FDR} = 2.91 \times 10^{-7}$), and the *M5* module is associated with blood vessel development and is enriched in the endothelial downregulated DEGs (OR = 3.91, $p_{FDR} = 4.43 \times 10^{-12}$) (Fig. 2b). The only exception to this is the *M1* module, which is associated with protein translation and is enriched in three different cell types (Fig. 2a). Based on these findings, we focused on the M2 and M5 modules in microglia and endothelial cells, respectively (Fig. 2).

2.2. Anti-angiogenic genes are downregulated in AD+Vas compared to other AD groups

The downregulated DEGs in endothelial cells are enriched for genes in the M5 module, which are linked to blood vessel ($p_{FDR} = 7.25 \times 10^{-4}$) and vascular ($p_{FDR} = 1.08 \times 10^{-3}$) development pathways (Fig. 2, Table 1). To further investigate the nature of the enriched genes, we examined the overlap of genes in this module with endothelial DEGs and observed a consistent pattern of downregulation (Fig. 3a). We designated the group of overlapping genes as endothelial anti-angiogenic genes (EAAGs). The sample-level expression of these EAAGs was aggregated into a single score for each individual, which revealed that this group of genes is significantly downregulated ($t = -4.84$, $p = 1.49 \times 10^{-3}$) (Fig. 3b). This downregulation of EAAGs is in alignment with the increased presence of arterial endothelial cells in samples with AD+Vas pathology (Supplemental Fig. 1). The expression of EAAGs was also positively correlated with the endothelial expression of anti-angiogenic (An et al., 2009; Chlenski et al., 2010) genes *RGCC* and *SPARC* (Supplemental Fig. 3).

2.3. Microglial activation is downregulated in AD+Vas compared to other AD groups

Genes in the M2 module, which are associated with immune system processes, are enriched in the downregulated DEGs of microglia (Fig. 2, Table 1). To identify the genes that primarily account for this signal, we further examined the microglial DEGs in the M2 module. Most of these genes were downregulated in AD+Vas samples, thus accounting for the signal shown in Fig. 2. However, two genes - *CX3CR1* and *P2RY12* - were upregulated, and their expression was generally opposite to expression of all other DEGs in this group (Fig. 4a). Results from GO analysis indicated that the downregulated genes in this module are primarily associated with microglial activation, including functions of macrophage activation ($p_{FDR} = 4.71 \times 10^{-5}$) and positive regulation of immune system processes ($p_{FDR} = 1.45 \times 10^{-4}$). The upregulated genes, by contrast, are primarily associated with regulation of microglial migration ($p_{FDR} = 4.96 \times 10^{-5}$) (Fig. 4a). Because *CX3CR1* and *P2RY12*, the two upregulated genes of the M2 module, are markers of HOM and are absent or heavily downregulated in LDAM (Haney et al., 2024), it is important to rule out that these differences are not the result of differences in the proportion of LDAM. Results from DEG analysis restricted to HOM were nearly identical to those from the analysis including all microglia (Supplemental Fig. 4), suggesting that this pattern is not due to different LDAM proportions among samples. Due to the differing expression patterns of upregulated and downregulated M2 module DEGs, we divided these genes into separate gene sets. Most of the genes are downregulated genes and are linked to microglial activation (Fig. 4a), which we designate as positive microglial activation genes (pMAGs). The only upregulated genes, *CX3CR1* and *P2RY12*, are microglial receptors known to negatively regulate microglial activation (Haynes et al., 2006; Lyons et al., 2009; Mildner et al., 2017; Zujovic et al., 2000), and thus designated as negative microglial activation genes (nMAGs). Comparison of aggregated expression of genes in the nMAG and pMAG sets using HOM nuclei between AD+Vas and other AD samples revealed a significant downregulation of pMAGs ($t = -2.67$, $p = 2.72 \times 10^{-2}$) and a suggestive upregulation of nMAGs ($t = 2.07$, $p = 6.94 \times 10^{-2}$) (Fig. 4b). Additionally, nMAG and pMAG expression scores were negatively correlated ($r = -0.87$, $p = 1.70 \times 10^{-2}$) (Fig. 4c).

2.4. Expression of endothelial angiogenesis and microglial immune genes is correlated

Given the disproportionate number of microglial and endothelial DEGs downregulated in AD+Vas samples (Fig. 1b,c), we investigated the associations between gene sets across the two cell types. The EAAG score was significantly associated with both the pMAG ($r = 0.68$, $p = 1.63 \times 10^{-3}$) and nMAG scores of microglial activation ($r = -0.57$, $p = 1.83 \times 10^{-2}$) (Fig. 3c). These findings were supported by the analysis of gene set scores derived from HOM (Supplemental Figs. 5 and 6) and endothelial cells identified in the ROSMAP snRNA-seq dataset. Specifically, significant negative associations with the same effect directions were observed between nMAG and pMAG scores ($r = -0.60$, $p = 3.67 \times 10^{-38}$) (Fig. 5a) and between the EAAG score and the pMAG ($r = 0.34$, $p = 8.37 \times 10^{-12}$) and nMAG ($r = -0.41$, $p = 2.31 \times 10^{-16}$) scores (Fig. 5a).

2.5. Replication of differential expression of key microglial genes in ROSMAP dataset

Of the 263 DEGs discovered in the microglial Boston University Alzheimer's Disease Research Center (BU-ADRC) dataset, 22 were differentially expressed in the ROSMAP dataset, with 20 of these showing the same direction of effect. Only *BASP1* and *MVB12B* showed opposing effect directions in the two datasets. Microglial expression of *P2RY12* was elevated in AD+Vas samples in the ROSMAP dataset ($z = 5.82$, $p_{FDR} = 8.73 \times 10^{-6}$). By contrast, despite the high correlation of *CX3CR1* and *P2RY12* expression (Supplemental Fig. 7), *CX3CR1* was not differentially expressed in AD+Vas subjects compared to the other AD subjects ($z = 2.41$, $p_{FDR} = 0.59$).

3. Discussion

In this study, we identified sets of genes that are differentially expressed between AD brains with coexisting vascular pathology and AD brains without vascular pathologies, including those with no additional or other pathologies. These gene sets are associated primarily with angiogenesis in endothelial cells and immune activation in microglia. Among the microglial activation genes (MAGs), there is a stratified pattern of expression in AD+Vas brain such that genes that negatively regulate microglia activation (nMAG) are more highly expressed and genes that positively regulate microglia activation (pMAG) are downregulated. We found that nMAGs are composed of two receptors, *CX3CR1* and *P2RY12*, which are positively associated with microglial migration (Fig. 4) and ubiquitously expressed in homeostatic microglia (Deczkowska et al., 2018). Their expression is negatively associated with the expression of pMAGs. The pMAGs by contrast are composed of genes which are positively associated with microglial immune activation. We demonstrated a reproducible negative association between these two gene sets which is consistent with previous studies showing *CX3CR1* and *P2RY12* negatively regulate microglial activation (Haynes et al., 2006; Lyons et al., 2009; Mildner et al., 2017; Zujovic et al., 2000).

In endothelial cells we observed the downregulation of genes which are associated with angiogenesis. However, how these genes regulate angiogenesis is less clear. Several genes, including *SRGN* and *APOLD1*, are positively associated with angiogenesis (Fan et al., 2023; Reine et al., 2015; Stritt et al., 2023; Tanaka et al., 2022; Yan et al., 2022) while others, including *ADAMTS9* and *SEMA3F*, are anti-angiogenic (Feng et al., 2022; Guo

et al., 2013; Koo et al., 2010; Lo et al., 2010; Neufeld et al., 2012; Sakurai et al., 2012). Among more highly ranked DEGs in our study, *ANGPT2* was the most significant DEG in endothelial cells and was also strongly downregulated in brain tissue exhibiting AD+Vas pathology. Its action is context-dependent (Souma et al., 2018), acting as a pro-angiogenic agonist of the protein kinase *TIE2* in the absence of vascular endothelial protein tyrosine phosphatase (*VEPTP*) and an anti-angiogenic antagonist in the presence of *VEPTP*. *VEPTP* is ubiquitously expressed in vascular endothelial cells (Vestweber, 2021), making *ANGPT2* anti-angiogenic in the context of vascular brain endothelial cells. Several other of the top-ranked DEGs, including *ADAMTS9, RGCC* and *SPARC* are also anti-angiogenic (An et al., 2009; Chlenski et al., 2010). Although *RGCC* and *SPARC* are not EAAGs in the strict sense, their expression was strongly correlated with the EAAGs (Supplemental Fig. 3), suggesting that they occur as part of a shared biological process. Our finding of a disproportionate representation of anti-angiogenic genes among the top DEGs suggests that the greater group of EAAGs is anti-angiogenic. The anti-angiogenic nature of these genes is further supported by our finding of a higher proportion of arterial endothelial cells in AD+Vas individuals, which may be caused by the downregulation of EAAGs (Supplemental Fig. 1).

We also identified a significant association of the expression of immune activation genes in microglia and the expression of angiogenesis genes in endothelial cells. EAAGs are negatively associated with angiogenesis and correlated with the expression of microglial activation genes. In particular, expression of EAAGs was associated with reduced expression nMAGs and higher expression of pMAGs. These patterns suggest that endothelial angiogenesis and microglial migration are positively correlated, as well as an antagonistic relationship between angiogenesis and microglial activation. Both *P2RY12* and *CX3CR1* are important for microglial migration (Cao et al., 2019; Chidambaram et al., 2020; Wolf et al., 2013), i.e. moving them along a chemical gradient towards their respective ligands. *P2RY12* is of particular interest because its expression has been linked to microglial closure of the blood-brain barrier (BBB) at sites of injury (Lou et al., 2016) and is required for the attachment of microglia to capillary walls (Bisht et al., 2021). This suggests that damaged endothelial cells may be recruiting microglia by releasing ligands to *P2RY12* and *CX3CR1* and leading microglia to close sites of damage.

How this process relates to angiogenesis is less clear. Microglia migrating towards the BBB have been shown to upregulate genes associated with the “regulation of vascular development and angiogenesis” (Habashy et al., 2023) which suggests that microglia may induce angiogenic effects on their associated vessels. *CX3CR1* and *P2RY12* expression has also been associated with angiogenesis. For example, in blood, *CX3CR1*+ monocytes promote aortic angiogenesis more than their *CX3CR1*− counterparts (Kim et al., 2016) and the use of *P2RY12*-inhibitors has been shown to be anti-angiogenic in vivo (Wang, 2021). Therefore, it is reasonable to expect similar behavior at the microglia-endothelial cell interface in the brain. Taken together, these findings suggest that the relationship may partially be explained by microglia inducing angiogenesis in endothelial cells, with differences in the expression of MAGs being caused by damaged endothelial cells releasing ligands to *CX3CR1* and *P2RY12*, thus promoting microglial chemotaxis and inhibiting microglial activation (Fig. 6). BBB dysfunction has been linked to AD+Vas (Barisano et al., 2022; Gong and Jia, 2022; Hussain et al., 2021; Tayler et al., 2021; Ueno et al., 2016) and

our data suggest that this dysfunction may be more evident in patients with mixed AD+Vas pathology.

Microglia may also play a role in modulating cerebral blood flow (CBF) in patients with AD+Vas. Recent studies have found that vessel-associated microglia can regulate local CBF (Bisht et al., 2021; Császár et al., 2022). In particular, the ablation of microglia has been shown to increase CBF of the brain vasculature in a *P2RY12*-dependent manner. This suggests that microglia exert an inhibitory role on CBF, with *P2RY12* contributing to this effect in parallel with its potential role in promoting endothelial angiogenesis. A similar pattern has been observed in perivascular macrophages in mouse muscle, with macrophages regulating blood flow to ischaemic muscle (Vågesjö et al., 2021). This is important because low cerebral blood flow has been associated with an increased risk of developing dementia (Schuff et al., 2009; Wolters et al., 2017), and this process may be worsened by the presence of increased vessel-associated microglia in AD+Vas individuals.

Microglia play a pivotal role in AD biology and have been associated with both AD risk and resistance (Olah et al., 2020). Dysfunctional microglia have been shown to worsen tau pathology (Leyns and Holtzman, 2017) and promote neurodegeneration by way of synaptic pruning (Leyns and Holtzman, 2017; Spangenberg and Green, 2017). However, microglia also have neuroprotective roles. For instance, they are instrumental in clearing amyloid-β aggregates in the brain and macrophages from carriers of the AD-associated *TREM2* R62H missense variant have impaired uptake of amyloid-β complexes (Spangenberg and Green, 2017). Our data suggest that, as a result of endothelial damage, microglia in the brains of AD+Vas individuals are more likely to be in a “surveillance state” whereby immune processes are downregulated and migration is promoted when compared to other individuals with AD. This suggests that the pro-inflammatory effect of microglia may have a smaller role in AD+Vas than in other pathological forms of AD.

Our study has noteworthy limitations. Many of our findings were generated from snRNAseq data, and expression of some AD-associated microglial genes is depleted in single-nucleus RNAseq experiments compared to single-cell RNAseq experiments (Thrupp et al., 2020). This issue, together with the relatively low microglial count in the data, could lead to an incomplete picture of microglial expression profiles. Another concern is that our results were derived from an analysis of a relatively small number of BU-ADRC samples, thus limiting the statistical power of the study. It is also noteworthy that we were unable to perform in-depth analyses of endothelial cell subtypes due to the limited number of arterial and venous endothelial cells in the dataset. Additionally, given the small number of available samples in the AD-only ($n = 3$) and AD+LBD ($n = 2$) groups, merging these groups increased statistical power while maintaining a vascular-pathology–negative comparator group and achieving a relatively balanced sample size ($n = 5$) compared to the AD+Vas group ($n = 6$). However, Lewy body pathology may introduce heterogeneity; larger, more finely stratified datasets would enable more precise separation of the effects of AD+LBD. Where sample sizes permit, we will perform additional analyses separating AD-only from AD+LBD to assess the robustness of our results and better isolate the impact of vascular pathology in our future study. Furthermore, we were unable to experimentally verify the status of microglial activation and angiogenesis in the post-mortem samples. Furthermore,

not all of the results were replicated; this may be due to expression differences between hippocampal and DLPFC tissue. Substantial expression differences between brain tissue types were observed in a schizophrenia study comparing expression between hippocampal and DLPFC tissue (Collado-Torres et al., 2019). Finally, the proposed connection between microglia and endothelial cells (Fig. 6) is based on correlations among pMAG, nMAG, and EAAG scores, which do not provide evidence of spatial proximity or directional signaling (e.g., from microglia to vasculature via *P2RY12*). Further studies using spatial transcriptomics or immunostaining are necessary to determine whether *P2RY12* expression localizes near blood vessels or colocalizes with endothelial markers.

In conclusion, we found evidence for an interaction between endothelial cells and microglia in human hippocampus tissue from persons with AD+Vas pathology. This relationship involves a gene expression profile associated with reduced immune activation and increased migration in microglia and angiogenesis in endothelial cells. Further studies of AD+Vas are needed to support and extend our findings.

4. Methods

4.1. Neuropathological evaluation

Tissue specimens for this study were obtained from BU-ADRC brain donors. A pathological diagnosis of AD was established using NIA-Reagan criteria to diagnose AD of intermediate or high likelihood (Newell et al., 1999). Other established criteria were used to diagnose the presence of brainstem, limbic, or neocortical Lewy body disease (Attems et al., 2021), hippocampal sclerosis (Blümcke et al., 2013), and frontotemporal lobar degeneration (Neary et al., 1998). Brain tissue was also evaluated for vascular pathology/disease, including the presence of old gross infarcts, old microinfarcts, old cerebral microbleeds, moderate-severe atherosclerosis of the Circle of Willis, and moderate-severe small vessel arteriolosclerosis in subcortical white or gray matter. Scores for pathologies rated on a none-mild-moderate-severe scale (atherosclerosis and arteriolosclerosis) were dichotomized as moderate/severe vs. none/mild. Among the 12 BU-ADRC brain donors included in our hippocampal snRNAseq profiling (AD-only = 3, AD+LBD = 2, AD+Vas = 6, non-AD control = 1), none of them had evidence of old cerebral microbleeds. Notably, all 6 CE+Vas brains exhibited moderate arteriolosclerosis in the subcortical white or gray matter; among these brains, five also showed old microinfarcts. The one non-AD pathological control had a Braak stage of 2, a CERAD score of 4 (indicating no neuritic plaque burden), and an MMSE score of 29 (Table 1). With respect to vascular pathology, the brain showed mild arteriolosclerosis, no atherosclerosis, and no old cerebral microbleeds, but did contain old infarcts. Accordingly, this case was classified as vascular disease without AD, dementia, or other neuropathologies, and was used as a control to examine single-cell level transcriptional changes associated with vascular pathology in the context of AD, the primary focus of this study.

4.2. Bulk RNA sequencing and data processing

Paired-end bulk RNA-sequencing (RNAseq) was performed using RNA extracted from 207 frozen hippocampal samples in the BU-ADRC brain tissue repository using the Illumina Truseq3 protocol. These samples included pathologically confirmed AD cases with or

without coexisting pathologies and controls who lacked evidence of neurodegenerative disease but may have had modest vascular pathologies (Supplemental Table 1 and Table 2). Adaptor removal was performed using Trimmomatic v0.39 (Bolger et al., 2014) and trimmed reads were aligned to the GRCh38 reference genome using the STAR aligner v2.7.10a STAR: Ultrafast Universal RNA-Seq Aligner, 2025). Gene level RNA quantification was done using RSEM v1.3.3 (Li and Dewey, 2011) expected count values. The filterByExpr function from edgeR v3.34.1 (Robinson et al., 2010) was applied with default settings to exclude genes with low expected read counts. The expected count matrix was normalized into a log-counts per million matrix using the logcpm function from edgeR with default settings. Principal component analysis performed using the prcomp function in R v4.1.1 revealed an outlier cluster which was not associated with any external variable (Supplemental Fig. 8, Supplemental Table 2). After excluding these outliers, 191 samples (73 with AD only pathology, 54 with AD+LBD pathology, 43 with AD+Vas pathology, 3 with AD pathology and hippocampal sclerosis, 1 with AD pathology and frontotemporal lobar degeneration, and 17 with little evidence of AD pathology) remained (Table 2), including 42 males and 149 females. Gene co-expression clusters were identified from analysis of the RNA-seq data for the 174 CE cases in this group using the weighted gene co-expression network analysis (WGCNA) software v1.71 (Fig. 7) (Langfelder and Horvath, 2008) (Supplemental Fig. 8). The “bicor” function was used to calculate the correlation matrix and genes were subsequently grouped into modules using the dynamicTreeCut function. These modules were then merged into larger units based on eigengene correlation using the mergeCloseModules function.

4.3. Single nucleus RNA sequencing data, processing, and quality control

Among the 207 frozen human hippocampal samples collected by the BU-ADRC with bulk RNAseq data, 16 samples were selected to perform snRNAseq of 5000–8000 nuclei per sample using the 10× Genomics Chromium™ platform. These samples were chosen because they had the highest RNA and sequencing quality among the original set of bulk RNAseq samples, and were enriched for individuals with AD+Vas. 30–50 mg tissue material was collected from fresh frozen brain hippocampus, to obtain approximately 2 million nuclei per donor using an established protocol (Fujita et al., 2022). Nuclei were isolated with EZ PREP buffer, followed by homogenization by a glass dounce tissue grinder. Nuclei were then centrifuged at 500 x*g* for 5 min at 4 °C. The isolated nuclei were suspended in 50–70 uL of nuclei suspension buffer, depending on pellet size, and filtered through a 35 μm cell strainer. Nuclei were quantified using AO/PI, with a final target of 5000–8000 nuclei for the 10× Genomics Chromium™ Single Cell Gene Expression protocol. Libraries were pooled and sequenced using an Illumina Nex-Seq2000 platform at the Boston University Single Cell Sequencing Core. The snRNAseq data from four samples were excluded because of their aberrant cell type composition. Over 90 % of the nuclei from these samples are part of a cell cluster that is extremely rare or absent in other samples (Supplemental Fig. 9a-b). Based on its unique high expression of *PAX6* and low expression of neuron-associated *GRIN2B*, we classified these cells as granule neuron progenitor cells (Luo et al., 2021) (Supplemental Fig. 9c). This cell type is unlikely to be naturally present at such high proportions. The remaining samples included 11 of the 174 individuals with bulk RNAseq data and a neuropathological diagnosis of AD and one individual among the 17 controls with bulk RNAseq data (Table 3).

Among the AD subjects, three had no other pathology, six had Vas pathology, and two had LBD pathology.

Publicly available snRNAseq data derived from the dorsolateral prefrontal cortex (DLPFC) of 393 Religious Orders Study and Memory and Aging Project (ROSMAP) participants (Fujita et al., 2022) were obtained to replicate gene co-expression findings, which included 119 males and 274 females. Samples were grouped into AD only, AD+LBD, and AD+Vas groups using the same criteria as the BU-ADRC individuals. A total of 118 subjects, including 33 males and 85 females, with AD+LBD (n = 10), AD+Vas (n = 89), and AD-only (n = 19) pathology were retained for further analysis after excluding samples with no AD pathology or pathology associated with other neurodegenerative diseases.

snRNAseq reads from both datasets were aligned using CellRanger v6.0.1. Quality control metrics were calculated with singleCellTK v2.6.0, using the DecontX (Yang et al., 2020) method to quantify ambient RNA contamination and the CxdsBcdsHyrbid (Bais and Kostka, 2020; Hong et al., 2022) method to identify doublets. Nuclei that had less than 250 UMIs or 500 genes, more than 5 % mitochondrial reads, or ambient RNA contamination scores higher than 0.5, and those identified as doublets were removed. Seurat (Butler et al., 2018) was used to normalize and cluster the nuclei in both datasets. Cell type classification was first performed on a subset of cells using a set of marker genes for seven cell types (Supplemental Table 3). Seurat clusters with high expression of each set of markers were classified as the corresponding cell type (Fig. 7). singleR v2.2.0 (Aran et al., 2023; Aran et al., 2019) was used for further classification of other cells, with the manually classified cells used as prior biological knowledge to identify cell types without manually interpreting clusters and defining marker genes multiple times. Cell types were further reclassified into more appropriate cell types on a case-by-case basis to improve the accuracy and granularity of cell typing (Supplemental Fig. 10). Cell clusters that were exclusively found in one sample were removed.

4.4. snRNAseq differential gene expression analysis

Differential gene expression between the AD+Vas pathology samples and the other samples classified as AD only or AD+LBD (hereafter referred to as “other AD”) was performed using the Seurat FindMarkers function. A two-sided Fisher’s exact test was performed to evaluate the overrepresentation of different co-expression modules, using the status of differentially expressed gene (DEG) and module inclusion as binary categories for the contingency table (Fig. 7). This process was performed separately for DEGs which were upregulated and downregulated in samples from persons with AD+Vas pathology. WGCNA modules derived from the 174 bulk RNAseq samples that had an adjusted p-value less than 0.01 and contained more than 50 genes were included in the analysis.

4.5. Scoring of gene sets and gene set replication

Gene set enrichment scores were calculated using expression data averaged in each cell type derived from the Seurat AverageExpression function and the combined z-scores method (Lee et al., 2008). Gene sets derived from the BU-ADRC data were scored with the ROSMAP snRNAseq average expression data for replication analyses. Linear regression was

performed to find associations of gene set scores derived from the BU-ADRC and ROSMAP expression datasets. ROSMAP data were analyzed with a model including covariates for age at death, sex, population group, years of education and post-mortem interval (PMI). BU-ADRC data were analyzed with a similar model but without covariates for education which is not available. Two-sided *t*-tests were used to assess differences between samples with AD+Vas pathology and the other AD samples. Gene ontology (GO) analysis was performed for all gene sets using g:Profiler (Reimand et al., 2007) with default settings. To prioritize the genes driving the enrichment signal, gene sets were obtained by overlapping the DEGs for a particular cell type with genes in the WGCNA modules enriched in the same cell type (Fig. 7). Replication analyses were performed using the much larger ROSMAP snRNAseq data allowed for the testing of a more complicated model for assessing transcriptional changes and characterizing heterogeneity in snRNAseq data using MAST (Finak et al., 2015) including covariates for age, sex, PMI, and the individual from which the cell was obtained.

Supplementary Material

Refer to Web version on PubMed Central for supplementary material.

Funding sources

This study was supported by National Institute on Aging grants R01-AG048927, U01-AG058654, U01-AG062602, U01-AG0772577, U01-081230, U01-AG082665, and P30-AG072978

Data availability

Raw and processed single nucleus RNAseq data from the ROSMAP samples can be obtained from the Synapse website (https://www.synapse.org/Synapse:syn31512863). Access to raw data derived from the BU-ADRC samples will be made available upon request.

Appendix A. Supplementary data

Supplementary data to this article can be found online at https://doi.org/10.1016/j.nbd.2025.107128.

References

An X, Jin Y, Guo H, Foo S-Y, Cully BL, Wu J, Zeng H, Rosenzweig A, Li J, 2009. Response gene to complement 32, a novel hypoxia-regulated angiogenic inhibitor. Circulation 120, 617–627. 10.1161/CIRCULATIONAHA.108.841502. [PubMed: 19652095]

Aran D, Looney AP, Liu L, Wu E, Fong V, Hsu A, Chak S, Naikawadi RP, Wolters PJ, Abate AR, Butte AJ, Bhattacharya M, 2019. Reference-based analysis of lung single-cell sequencing reveals a transitional profibrotic macrophage. Nat. Immunol 20, 163–172. 10.1038/s41590-018-0276-y. [PubMed: 30643263]

Aran D, Lun A, Bunis D, Andrews J, Dündar F, 2023. SingleR: Reference-Based Single-Cell RNA-Seq Annotation. 10.18129/B9.bioc.SingleR.

Attems J, Toledo JB, Walker L, Gelpi E, Gentleman S, Halliday G, Hortobagyi T, Jellinger K, Kovacs GG, Lee EB, Love S, McAleese KE, Nelson PT, Neumann M, Parkkinen L, Polvikoski T, Sikorska B, Smith C, Grinberg LT, Thal DR, Trojanowski JQ, McKeith IG, 2021. Neuropathological

consensus criteria for the evaluation of Lewy pathology in post-mortem brains: a multi-Centre study. Acta Neuropathol. (Berl.) 141, 159–172. 10.1007/s00401-020-02255-2. [PubMed: 33399945]

Bais AS, Kostka D, 2020. Scds: computational annotation of doublets in single-cell RNA sequencing data. Bioinforma. Oxf. Engl 36, 1150–1158. 10.1093/bioinformatics/btz698.

Barisano G, Montagne A, Kisler K, Schneider JA, Wardlaw JM, Zlokovic BV, 2022. Blood-brain barrier link to human cognitive impairment and Alzheimer's disease. Nat. Cardiovasc. Res 1, 108–115. 10.1038/s44161-021-00014-4. [PubMed: 35450117]

Bellenguez C, Küçükali F, Jansen IE, Kleineidam L, Moreno-Grau S, Amin N, Naj AC, Campos-Martin R, Grenier-Boley B, Andrade V, Holmans PA, Boland A, Damotte V, van der Lee SJ, Costa MR, Kuulasmaa T, Yang Q, de Rojas I, Bis JC, Yaqub A, Prokic I, Chapuis J, Ahmad S, Giedraitis V, Aarsland D, Garcia-Gonzalez P, Abdelnour C, Alarcón-Martín E, Alcolea D, Alegret M, Alvarez I, Álvarez V, Armstrong NJ, Tsolaki A, Antúnez C, Appollonio I, Arcaro M, Archetti S, Pastor AA, Arosio B, Athanasiu L, Bailly H, Banaj N, Baquero M, Barral S, Beiser A, Pastor AB, Below JE, Benchek P, Benussi L, Berr C, Besse C, Bessi V, Binetti G, Bizarro A, Blesa R, Boada M, Boerwinkle E, Borroni B, Boschi S, Bossù P, Bråthen G, Bressler J, Bresner C, Brodaty H, Brookes KJ, Brusco LI, Buiza-Rueda D, Bûrger K, Burholt V, Bush WS, Calero M, Cantwell LB, Chene G, Chung J, Cuccaro ML, Carracedo Á, Cecchetti R, Cervera-Carles L, Charbonnier C, Chen H-H, Chillotti C, Ciccone S, Claassen JAHR, Clark C, Conti E, Corma-Gómez A, Costantini E, Custodero C, Daian D, Dalmasso MC, Daniele A, Dardiotis E, Dartigues J-F, de Deyn PP, de Paiva Lopes K, de Witte LD, Debette S, Deckert J, del Ser T, Denning N, DeStefano A, Dichgans M, Diehl-Schmid J, Diez-Fairen M, Rossi PD, Djurovic S, Duron E, Düzel E, Dufouil C, Eiriksdottir G, Engelborghs S, Escott-Price V, Espinosa A, Ewers M, Faber KM, Fabrizio T, Nielsen SF, Fardo DW, Farotti L, Fenoglio C, Fernández-Fuertes M, Ferrari R, Ferreira CB, Ferri E, Fin B, Fischer P, Fladby T, Fließbach K, Fongang B, Fornage M, Fortea J, Foroud TM, Fostinelli S, Fox NC, Franco-Macías E, Bullido MJ, Frank-García A, Froelich L, Fulton-Howard B, Galimberti D, García-Alberca JM, García-González P, Garcia-Madrona S, Garcia-Ribas G, Ghidoni R, Giegling I, Giorgio G, Goate AM, Goldhardt O, Gomez-Fonseca D, González-Pérez A, Graff C, Grande G, Green E, Grimmer T, Grünblatt E, Grunin M, Gudnason V, Guetta-Baranes T, Haapasalo A, Hadjigeorgiou G, Haines JL, Hamilton-Nelson KL, Hampel H, Hanon O, Hardy J, Hartmann AM, Hausner L, Harwood J, Heilmann-Heimbach S, Helisalmi S, Heneka MT, Hernández I, Herrmann MJ, Hoffmann P, Holmes C, Holstege H, Vilas RH, Hulsman M, Humphrey J, Biessels GJ, Jian X, Johansson C, Jun GR, Kastumata Y, Kauwe J, Kehoe PG, Kilander L, Ståhlbom AK, Kivipelto M, Koivisto A, Kornhuber J, Kosmidis MH, Kukull WA, Kuksa PP, Kunkle BW, Kuzma AB, Lage C, Laukka EJ, Launer L, Lauria A, Lee C-Y, Lehtisalo J, Lerch O, Lleó A, Longstreth W, Lopez O, de Munain AL, Love S, Löwemark M, Luckcuck L, Lunetta KL, Ma Y, Macías J, MacLeod CA, Maier W, Mangialasche F, Spallazzi M, Marquié M, Marshall R, Martin ER, Montes AM, Rodríguez CM, Masullo C, Mayeux R, Mead S, Mecocci P, Medina M, Meggy A, Mehrabian S, Mendoza S, Menéndez-González M, Mir P, Moebus S, Mol M, Molina-Porcel L, Montrreal L, Morelli L, Moreno F, Morgan K, Mosley T, Nöthen MM, Muchnik C, Mukherjee S, Nacmias B, Ngandu T, Nicolas G, Nordestgaard BG, Olaso R, Orellana A, Orsini M, Ortega G, Padovani A, Paolo C, Papenberg G, Parnetti L, Pasquier F, Pastor P, Peloso G, Pérez-Cordón A, Pérez-Tur J, Pericard P, Peters O, Pijnenburg YAL, Pineda JA, Piñol-Ripoll G, Pisanu C, Polak T, Popp J, Posthuma D, Priller J, Puerta R, Quenez O, Quintela I, Thomassen JQ, Rábano A, Rainero I, Rajabli F, Ramakers I, Real LM, Reinders MJT, Reitz C, Reyes-Dumeyer D, Ridge P, Riedel-Heller S, Riederer P, Roberto N, Rodriguez-Rodriguez E, Rongve A, Allende IR, Rosende-Roca M, Royo JL, Rubino E, Rujescu D, Sáez ME, Sakka P, Saltvedt I, Sanabria Á, Sánchez-Arjona MB, Sanchez-Garcia F, Juan PS, Sánchez-Valle R, Sando SB, Sarnowski C, Satizabal CL, Scamosci M, Scarmeas N, Scarpini E, Scheltens P, Scherbaum N, Scherer M, Schmid M, Schneider A, Schott JM, Selbæk G, Seripa D, Serrano M, Sha J, Shadrin AA, Skrobot O, Slifer S, Snijders GJL, Soininen H, Solfrizzi V, Solomon A, Song Y, Sorbi S, Sotolongo-Grau O, Spalletta G, Spottke A, Squassina A, Stordal E, Tartan JP, Tárraga L, Tesí N, Thalamuthu A, Thomas T, Tosto G, Traykov L, Tremolizzo L, Tybjærg-Hansen A, Uitterlinden A, Ullgren A, Ulstein I, Valero S, Valladares O, Broeckhoven CV, Vance J, Vardarajan BN, van der Lugt A, Dongen JV, van Rooij J, van Swieten J, Vandenberghe R, Verhey F, Vidal J-S, Vogelgsang J, Vyhnalek M, Wagner M, Wallon D, Wang L-S, Wang R, Weinhold L, Wiltfang J, Windle G, Woods B, Yannakoulia M, Zare H, Zhao Y, Zhang X, Zhu C, Zulaica M, Farrer LA, Psaty BM, Ghanbari M, Raj T, Sachdev P, Mather K, Jessen F, Ikram MA, de Mendonça A, Hort J, Tsolaki M, Pericak-Vance MA, Amouyel P, Williams J, Frikke-Schmidt R,

Clarimon J, Deleuze J-F, Rossi G, Seshadri S, Andreassen OA, Ingelsson M, Hiltunen M, Sleegers K, Schellenberg GD, van Duijn CM, Sims R, van der Flier WM, Ruiz A, Ramirez A, Lambert J-C, 2022. New insights into the genetic etiology of Alzheimer's disease and related dementias. Nat. Genet 54, 412–436. 10.1038/s41588-022-01024-z. [PubMed: 35379992]

Bisht K, Okojie KA, Sharma K, Lentferink DH, Sun Y-Y, Chen H-R, Uweru JO, Amancherla S, Calcuttawala Z, Campos-Salazar AB, Corliss B, Jabbour L, Benderoth J, Friestad B, Mills WA, Isakson BE, Tremblay M-È, Kuan C-Y, Eyo UB, 2021. Capillary-associated microglia regulate vascular structure and function through PANX1-P2RY12 coupling in mice. Nat. Commun 12, 5289. 10.1038/s41467-021-25590-8. [PubMed: 34489419]

Blümcke I, Thom M, Aronica E, Armstrong DD, Bartolomei F, Bernasconi A, Bernasconi N, Bien CG, Cendes F, Coras R, Cross JH, Jacques TS, Kahane P, Mathern GW, Miyata H, Moshé SL, Oz B, Özkara Ç, Perucca E, Sisodiya S, Wiebe S, Spreafico R, 2013. International consensus classification of hippocampal sclerosis in temporal lobe epilepsy: A task force report from the ILAE commission on diagnostic methods. Epilepsia 54, 1315–1329. 10.1111/epi.12220. [PubMed: 23692496]

Bolger AM, Lohse M, Usadel B, 2014. Trimmomatic: a flexible trimmer for Illumina sequence data. Bioinformatics 30, 2114–2120. 10.1093/bioinformatics/btu170. [PubMed: 24695404]

Boyle PA, Yu L, Wilson RS, Leurgans SE, Schneider JA, Bennett DA, 2018. Person-specific contribution of neuropathologies to cognitive loss in old age. Ann. Neurol 83, 74–83. 10.1002/ana.25123. [PubMed: 29244218]

Broce IJ, Tan CH, Fan CC, Jansen I, Savage JE, Witoelar A, Wen N, Hess CP, Dillon WP, Glastonbury CM, Glymour M, Yokoyama JS, Elahi FM, Rabinovici GD, Miller BL, Mormino EC, Sperling RA, Bennett DA, McEvoy LK, Brewer JB, Feldman HH, Hyman BT, Pericak-Vance M, Haines JL, Farrer LA, Mayeux R, Schellenberg GD, Yaffe K, Sugrue LP, Dale AM, Posthuma D, Andreassen OA, Karch CM, Desikan RS, 2019. Dissecting the genetic relationship between cardiovascular risk factors and Alzheimer's disease. Acta Neuropathol. (Berl.) 137, 209–226. 10.1007/s00401-018-1928-6. [PubMed: 30413934]

Butler A, Hoffman P, Smibert P, Papalexi E, Satija R, 2018. Integrating single-cell transcriptomic data across different conditions, technologies, and species. Nat. Biotechnol 36, 411–420. 10.1038/nbt.4096. [PubMed: 29608179]

Cao R, Li S, Yin J, Guo L, Shi J, 2019. Sirtuin 3 promotes microglia migration by upregulating CX3CR1. Cell Adhes. Migr 13, 229–235. 10.1080/19336918.2019.1629224.

Chidambaram H, Das R, Chinnathambi S, 2020. Interaction of tau with the chemokine receptor, CX3CR1 and its effect on microglial activation, migration and proliferation. Cell Biosci. 10, 109. 10.1186/s13578-020-00474-4. [PubMed: 32944223]

Chlenski A, Guerrero LJ, Peddinti R, Spitz JA, Leonhardt PT, Yang Q, Tian Y, Salwen HR, Cohn SL, 2010. Anti-angiogenic SPARC peptides inhibit progression of neuroblastoma tumors. Mol. Cancer 9, 138. 10.1186/1476-4598-9-138. [PubMed: 20525313]

Collado-Torres L, Burke EE, Peterson A, Shin J, Straub RE, Rajpurohit A, Semick SA, Ulrich WS, Consortium, BrainSeq, Price AJ, Valencia C, Tao R, Deep-Soboslay A, Hyde TM, Kleinman JE, Weinberger DR, Jaffe AE, 2019. Regional heterogeneity in gene expression, regulation, and coherence in the frontal cortex and Hippocampus across development and schizophrenia. Neuron 103, 203–216 e8. 10.1016/j.neuron.2019.05.013. [PubMed: 31174959]

Crehan H, Hardy J, Pocock J, 2013. Blockage of CR1 prevents activation of rodent microglia. Neurobiol. Dis 54, 139–149. 10.1016/j.nbd.2013.02.003. [PubMed: 23454195]

Császár E, Lénárt N, Cserép C, Környei Z, Fekete R, Pósfai B, Balázsfi D, Hangya B, Schwarcz AD, Szabadits E, Szöllősi D, Szigeti K, Máthé D, West BL, Sviatkó K, Brás AR, Mariani J-C, Kliewer A, Lenkei Z, Hricisák L, Benyó Z, Baranyi M, Sperlágh B, Menyhárt Á, Farkas E, Dénes Á, 2022. Microglia modulate blood flow, neurovascular coupling, and hypoperfusion via purinergic actions. J. Exp. Med 219, e20211071. 10.1084/jem.20211071. [PubMed: 35201268]

Deczkowska A, Keren-Shaul H, Weiner A, Colonna M, Schwartz M, Amit I, 2018. Disease-associated microglia: a universal immune sensor of neurodegeneration. Cell 173, 1073–1081. 10.1016/j.cell.2018.05.003. [PubMed: 29775591]

Ding J, Adiconis X, Simmons SK, Kowalczyk MS, Hession CC, Marjanovic ND, Hughes TK, Wadsworth MH, Burks T, Nguyen LT, Kwon JYH, Barak B, Ge W, Kedaigle AJ, Carroll S, Li S, Hacohen N, Rozenblatt-Rosen O, Shalek AK, Villani A-C, Regev A, Levin JZ, 2020. Systematic

comparison of single-cell and single-nucleus RNA-sequencing methods. Nat. Biotechnol 38, 737–746. 10.1038/s41587-020-0465-8. [PubMed: 32341560]

Dzamba D, Harantova L, Butenko O, Anderova M, 2016. Glial cells - the key elements of Alzheimer's disease. Curr. Alzheimer Res 13, 894–911. 10.2174/1567205013666160129095924. [PubMed: 26825092]

Fan Z, Ardicoglu R, Batavia AA, Rust R, von Ziegler L, Waag R, Zhang J, Desgeorges T, Sturman O, Dang H, Weber R, Roszkowski M, Moor AE, Schwab ME, Germain P-L, Bohacek J, De Bock K, 2023. The vascular gene Apold1 is dispensable for normal development but controls angiogenesis under pathological conditions. Angiogenesis. 10.1007/s10456-023-09870-z.

Feleke R, Reynolds RH, Smith AM, Tilley B, Taliun SAG, Hardy J, Matthews PM, Gentleman S, Owen DR, Johnson MR, Srivastava PK, Ryten M, 2021. Cross-platform transcriptional profiling identifies common and distinct molecular pathologies in Lewy body diseases. Acta Neuropathol. (Berl.) 142, 449–474. 10.1007/s00401-021-02343-x. [PubMed: 34309761]

Feng N, Wang Zhengfei, Wu Y, Zheng H, Jiang X, Wang Zhi, Qu F, Zhang Z, 2022. ADAMTS9-AS2 promotes angiogenesis of brain microvascular endothelial cells through regulating miR-185-5p/IGFBP-2 Axis in ischemic stroke. Mol. Neurobiol 59, 2593–2604. 10.1007/s12035-021-02641-1. [PubMed: 35098480]

Finak G, McDavid A, Yajima M, Deng J, Gersuk V, Shalek AK, Slichter CK, Miller HW, McElrath MJ, Prlic M, Linsley PS, Gottardo R, 2015. MAST: a flexible statistical framework for assessing transcriptional changes and characterizing heterogeneity in single-cell RNA sequencing data. Genome Biol. 16, 278. 10.1186/s13059-015-0844-5. [PubMed: 26653891]

Fujita M, Gao Z, Zeng L, McCabe C, White CC, Ng B, Green GS, Rozenblatt-Rosen O, Phillips D, Amir-Zilberstein L, Lee H, Pearse RV, Khan A, Vardarajan BN, Kiryluk K, Ye CJ, Klein H-U, Wang G, Regev A, Habib N, Schneider JA, Wang Y, Young-Pearse T, Mostafavi S, Bennett DA, Menon V, Jager PLD, 2022. Cell-Subtype Specific Effects of Genetic Variation in the Aging and Alzheimer Cortex. 10.1101/2022.11.07.515446.

Gong M, Jia J, 2022. Contribution of blood-brain barrier-related blood-borne factors for Alzheimer's disease vs. vascular dementia diagnosis: a pilot study. Front. Neurosci 16.

Gottesman RF, Schneider ALC, Zhou Y, Coresh J, Green E, Gupta N, Knopman DS, Mintz A, Rahmim A, Sharrett AR, Wagenknecht LE, Wong DF, Mosley TH, 2017. Association between midlife vascular risk factors and estimated brain amyloid deposition. JAMA 317, 1443–1450. 10.1001/jama.2017.3090. [PubMed: 28399252]

Grindberg RV, Yee-Greenbaum JL, McConnell MJ, Novotny M, O'Shaughnessy AL, Lambert GM, Araúzo-Bravo MJ, Lee J, Fishman M, Robbins GE, Lin X, Venepally P, Badger JH, Galbraith DW, Gage FH, Lasken RS, 2013. RNA-sequencing from single nuclei. Proc. Natl. Acad. Sci. USA 110, 19802–19807. 10.1073/pnas.1319700110. [PubMed: 24248345]

Grubman A, Chew G, Ouyang JF, Sun G, Choo XY, McLean C, Simmons RK, Buckberry S, Vargas-Landin DB, Poppe D, Pflueger J, Lister R, Rackham OJL, Petretto E, Polo JM, 2019. A single-cell atlas of entorhinal cortex from individuals with Alzheimer's disease reveals cell-type-specific gene expression regulation. Nat. Neurosci 22, 2087–2097. 10.1038/s41593-019-0539-4. [PubMed: 31768052]

Guo H-F, Li X, Parker MW, Waltenberger J, Becker PM, Vander Kooi CW, 2013. Mechanistic basis for the potent anti-angiogenic activity of semaphorin 3F. Biochemistry 52, 7551–7558. 10.1021/bi401034q. [PubMed: 24079887]

Habashy K, Arrieta V, Luan Y, Kim K-S, Dhiantravan S, Najem H, Gomez M, Dmello C, Chen L, Saganty R, Gould A, Hou Y, Heimberger A, Canney M, Stupp R, Yue F, Sonabend A, 2023. DDEL-06. Microglia repair the disrupted blood-brain barrier following low-intensity pulsed ultrasound through p2ry12 signaling. Neuro-Oncology 25, v102. 10.1093/neuonc/noad179.0385.

Haney MS, Pálovics R, Munson CN, Long C, Johansson PK, Yip O, Dong W, Rawat E, West E, Schlachetzki JCM, Tsai A, Guldner IH, Lamichhane BS, Smith A, Schaum N, Calcuttawala K, Shin A, Wang Y-H, Wang C, Koutsodendris N, Serrano GE, Beach TG, Reiman EM, Glass CK, Abu-Remaileh M, Enejder A, Huang Y, Wyss-Coray T, 2024. APOE4/4 is linked to damaging lipid droplets in Alzheimer's disease microglia. Nature 628, 154–161. 10.1038/s41586-024-07185-7. [PubMed: 38480892]

Hansen DV, Hanson JE, Sheng M, 2018. Microglia in Alzheimer's disease. J. Cell Biol 217, 459–472. 10.1083/jcb.201709069. [PubMed: 29196460]

Haynes SE, Hollopeter G, Yang G, Kurpius D, Dailey ME, Gan W-B, Julius D, 2006. The P2Y12 receptor regulates microglial activation by extracellular nucleotides. Nat. Neurosci 9, 1512–1519. 10.1038/nn1805. [PubMed: 17115040]

Hong R, Koga Y, Bandyadka S, Leshchyk A, Wang Y, Akavoor V, Cao X, Sarfraz I, Wang Z, Alabdullatif S, Jansen F, Yajima M, Johnson WE, Campbell JD, 2022. Comprehensive generation, visualization, and reporting of quality control metrics for single-cell RNA sequencing data. Nat. Commun 13, 1688. 10.1038/s41467-022-29212-9. [PubMed: 35354805]

Hussain B, Fang C, Chang J, 2021. Blood–brain barrier breakdown: an emerging biomarker of cognitive impairment in normal aging and dementia. Front. Neurosci 15.

Jansen IE, Savage JE, Watanabe K, Bryois J, Williams DM, Steinberg S, Sealock J, Karlsson IK, Hägg S, Athanasiu L, Voyle N, Proitsi P, Witoelar A, Stringer S, Aarsland D, Almdahl IS, Andersen F, Bergh S, Bettella F, Bjornsson S, Brækhus A, Bråthen G, de Leeuw C, Desikan RS, Djurovic S, Dumitrescu L, Fladby T, Hohman TJ, Jonsson PV, Kiddle SJ, Rongve A, Saltvedt I, Sando SB, Selbæk G, Shoai M, Skene NG, Snaedal J, Stordal E, Ulstein ID, Wang Y, White LR, Hardy J, Hjerling-Leffler J, Sullivan PF, van der Flier WM, Dobson R, Davis LK, Stefansson H, Stefansson K, Pedersen NL, Ripke S, Andreassen OA, Posthuma D, 2019. Genome-wide meta-analysis identifies new loci and functional pathways influencing Alzheimer's disease risk. Nat. Genet 51, 404–413. 10.1038/s41588-018-0311-9. [PubMed: 30617256]

Kim JA, Kwak J-Y, Eunjung Y, Lee J, Park Y, Broxmeyer HE, 2016. Fractalkine/CX3CR1 signaling promotes angiogenic potentials in CX3CR1 expressing monocytes. Blood 128, 2507. 10.1182/blood.V128.22.2507.2507.

Kim YS, Jung HM, Yoon B-E, 2018. Exploring glia to better understand Alzheimer's disease. Anim. Cells Syst 22, 213–218. 10.1080/19768354.2018.1508498.

Koo B-H, Coe DM, Dixon LJ, Somerville RPT, Nelson CM, Wang LW, Young ME, Lindner DJ, Apte SS, 2010. ADAMTS9 is a cell-autonomously acting, anti-angiogenic metalloprotease expressed by microvascular endothelial cells. Am. J. Pathol 176, 1494–1504. 10.2353/ajpath.2010.090655. [PubMed: 20093484]

Kumar A, Sidhu J, Goyal A, Tsao JW, 2023. Alzheimer disease. In: StatPearls. StatPearls Publishing, Treasure Island (FL).

Kunkle BW, Grenier-Boley B, Sims R, Bis JC, Damotte V, Naj AC, Boland A, Vronskaya M, van der Lee SJ, Amlie-Wolf A, Bellenguez C, Frizatti A, Chouraki V, Martin ER, Sleegers K, Badarinarayan N, Jakobsdottir J, Hamilton-Nelson KL, Moreno-Grau S, Olaso R, Raybould R, Chen Y, Kuzma AB, Hiltunen M, Morgan T, Ahmad S, Vardarajan BN, Epelbaum J, Hoffmann P, Boada M, Beecham GW, Garnier J-G, Harold D, Fitzpatrick AL, Valladares O, Moutet M-L, Gerrish A, Smith AV, Qu L, Bacq D, Denning N, Jian X, Zhao Y, Del Zompo M, Fox NC, Choi S-H, Mateo I, Hughes JT, Adams HH, Malamon J, Sanchez-Garcia F, Patel Y, Brody JA, Dombroski BA, Naranjo MCD, Daniilidou M, Eiriksdottir G, Mukherjee S, Wallon D, Uphill J, Aspelund T, Cantwell LB, Garzia F, Galimberti D, Hofer E, Butkiewicz M, Fin B, Scarpini E, Sarnowski C, Bush WS, Meslage S, Kornhuber J, White CC, Song Y, Barber RC, Engelborghs S, Sordon S, Voijnovic D, Adams PM, Vandenberghe R, Mayhaus M, Cupples LA, Albert MS, De Deyn PP, Gu W, Himali JJ, Beekly D, Squassina A, Hartmann AM, Orellana A, Blacker D, Rodriguez-Rodriguez E, Lovestone S, Garcia ME, Doody RS, Munoz-Fernadez C, Sussams R, Lin H, Fairchild TJ, Benito YA, Holmes C, Karamujić-Čomić H, Frosch MP, Thonberg H, Maier W, Roshchupkin G, Ghetti B, Giedraitis V, Kawalia A, Li S, Huebinger RM, Kilander L, Moebus S, Hernández I, Kamboh MI, Brundin R, Turton J, Yang Q, Katz MJ, Concari L, Lord J, Beiser AS, Keene CD, Helisalmi S, Kloszewska I, Kukull WA, Koivisto AM, Lynch A, Tarraga L, Larson EB, Haapasalo A, Lawlor B, Mosley TH, Lipton RB, Solfrizzi V, Gill M, Longstreth WT, Montine TJ, Frisardi V, Diez-Fairen M, Rivadeneira F, Petersen RC, Deramecourt V, Alvarez I, Salani F, Ciaramella A, Boerwinkle E, Reiman EM, Fievet N, Rotter JI, Reisch JS, Hanon O, Cupidi C, Andre Uitterlinden AG, Royall DR, Dufouil C, Maletta RG, de Rojas I, Sano M, Brice A, Cecchetti R, George-Hyslop PS, Ritchie K, Tsolaki M, Tsuang DW, Dubois B, Craig D, Wu C-K, Soininen H, Avramidou D, Albin RL, Fratiglioni L, Germanou A, Apostolova LG, Keller L, Koutroumani M, Arnold SE, Panza F, Gkatzima O, Asthana S, Hannequin D, Whitehead P, Atwood CS, Caffarra P, Hampel H, Quintela I, Carracedo Á, Lannfelt L, Rubinsztein DC, Barnes

LL, Pasquier F, Frölich L, Barral S, McGuinness B, Beach TG, Johnston JA, Becker JT, Passmore P, Bigio EH, Schott JM, Bird TD, Warren JD, Boeve BF, Lupton MK, Bowen JD, Proitsi P, Boxer A, Powell JF, Burke JR, Kauwe JSK, Burns JM, Mancuso M, Buxbaum JD, Bonuccelli U, Cairns NJ, McQuillin A, Cao C, Livingston G, Carlson CS, Bass NJ, Carlsson CM, Hardy J, Carney RM, Bras J, Carrasquillo MM, Guerreiro R, Allen M, Chui HC, Fisher E, Masullo C, Crocco EA, DeCarli C, Bisceglio G, Dick M, Ma L, Duara R, Graff-Radford NR, Evans DA, Hodges A, Faber KM, Scherer M, Fallon KB, Riemenschneider M, Fardo DW, Heun R, Farlow MR, Kölsch H, Ferris S, Leber M, Foroud TM, Heuser I, Galasko DR, Giegling I, Gearing M, Hüll M, Geschwind DH, Gilbert JR, Morris J, Green RC, Mayo K, Growdon JH, Feulner T, Hamilton RL, Harrell LE, Drichel D, Honig LS, Cushion TD, Huentelman MJ, Hollingworth P, Hulette CM, Hyman BT, Marshall R, Jarvik GP, Meggy A, Abner E, Menzies GE, Jin L-W, Leonenko G, Real LM, Jun GR, Baldwin CT, Grozeva D, Karydas A, Russo G, Kaye JA, Kim R, Jessen F, Kowall NW, Vellas B, Kramer JH, Vardy E, LaFerla FM, Jöckel K-H, Lah JJ, Dichgans M, Leverenz JB, Mann D, Levey AI, Pickering-Brown S, Lieberman AP, Klopp N, Lunetta KL, Wichmann H-E, Lyketsos CG, Morgan K, Marson DC, Brown K, Martiniuk F, Medway C, Mash DC, Nöthen MM, Masliah E, Hooper NM, McCormick WC, Daniele A, McCurry SM, Bayer A, McDavid AN, Gallacher J, McKee AC, van den Bussche H, Mesulam M, Brayne C, Miller BL, Riedel-Heller S, Miller CA, Miller JW, Al-Chalabi A, Morris JC, Shaw CE, Myers AJ, Wiltfang J, O'Bryant S, Olichney JM, Alvarez V, Parisi JE, Singleton AB, Paulson HL, Collinge J, Perry WR, Mead S, Peskind E, Cribbs DH, Rossor M, Pierce A, Ryan NS, Poon WW, Nacmias B, Potter H, Sorbi S, Quinn JF, Sacchinelli E, Raj A, Spalletta G, Raskind M, Caltagirone C, Bossù P, Orfei MD, Reisberg B, Clarke R, Reitz C, Smith AD, Ringman JM, Warden D, Roberson ED, Wilcock G, Rogaeva E, Bruni AC, Rosen HJ, Gallo M, Rosenberg RN, Ben-Shlomo Y, Sager MA, Mecocci P, Saykin AJ, Pastor P, Cuccaro ML, Vance JM, Schneider JA, Schneider LS, Slifer S, Seeley WW, Smith AG, Sonnen JA, Spina S, Stern RA, Swerdlow RH, Tang M, Tanzi RE, Trojanowski JQ, Troncoso JC, Van Deerlin VM, Van Eldik LJ, Vinters HV, Vonsattel JP, Weintraub S, Welsh-Bohmer KA, Wilhelmsen KC, Williamson J, Wingo TS, Woltjer RL, Wright CB, Yu C-E, Yu L, Saba Y, Pilotto A, Bullido MJ, Peters O, Crane PK, Bennett D, Bosco P, Coto E, Boccardi V, De Jager PL, Lleo A, Warner N, Lopez OL, Ingelsson M, Deloukas P, Cruchaga C, Graff C, Gwilliam R, Fornage M, Goate AM, Sanchez-Juan P, Kehoe PG, Amin N, Ertekin-Taner N, Berr C, Debette S, Love S, Launer LJ, Younkin SG, Dartigues J-F, Corcoran C, Ikram MA, Dickson DW, Nicolas G, Campion D, Tschanz J, Schmidt H, Hakonarson H, Clarimon J, Munger R, Schmidt R, Farrer LA, Van Broeckhoven C, O'Donovan C, DeStefano AL, Jones L, Haines JL, Deleuze J-F, Owen MJ, Gudnason V, Mayeux R, Escott-Price V, Psaty BM, Ramirez A, Wang L-S, Ruiz A, van Duijn CM, Holmans PA, Seshadri S, Williams J, Amouyel P, Schellenberg GD, Lambert J-C, Pericak-Vance MA, 2019. Genetic meta-analysis of diagnosed Alzheimer's disease identifies new risk loci and implicates Aβ, tau, immunity and lipid processing. Nat. Genet 51, 414–430. 10.1038/s41588-019-0358-2. [PubMed: 30820047]

Langfelder P, Horvath S, 2008. WGCNA: an R package for weighted correlation network analysis. BMC Bioinform. 9, 559. 10.1186/1471-2105-9-559.

Lau S-F, Cao H, Fu AKY, Ip NY, 2020. Single-nucleus transcriptome analysis reveals dysregulation of angiogenic endothelial cells and neuroprotective glia in Alzheimer's disease. Proc. Natl. Acad. Sci 117, 25800–25809. 10.1073/pnas.2008762117. [PubMed: 32989152]

Lee E, Chuang H-Y, Kim J-W, Ideker T, Lee D, 2008. Inferring pathway activity toward precise disease classification. PLoS Comput. Biol 4, e1000217. 10.1371/journal.pcbi.1000217. [PubMed: 18989396]

Lee S, Devanney NA, Golden LR, Smith CT, Schwartz JL, Walsh AE, Clarke HA, Goulding DS, Allenger EJ, Morillo-Segovia G, Friday CM, Gorman AA, Hawkinson TR, MacLean SM, Williams HC, Sun RC, Morganti JM, Johnson LA, 2023. APOE modulates microglial immunometabolism in response to age, amyloid pathology, and inflammatory challenge. Cell Rep. 42, 112196. 10.1016/j.celrep.2023.112196. [PubMed: 36871219]

Leyns CEG, Holtzman DM, 2017. Glial contributions to neurodegeneration in tauopathies. Mol. Neurodegener 12, 50. 10.1186/s13024-017-0192-x. [PubMed: 28662669]

Li B, Dewey CN, 2011. RSEM: accurate transcript quantification from RNA-Seq data with or without a reference genome. BMC Bioinform. 12, 323. 10.1186/1471-2105-12-323.

Lo PHY, Lung HL, Cheung AKL, Apte SS, Chan KW, Kwong FM, Ko JMY, Cheng Y, Law S, Srivastava G, Zabarovsky ER, Tsao SW, Tang JCO, Stanbridge EJ, Lung ML, 2010. Extracellular protease ADAMTS9 suppresses esophageal and nasopharyngeal carcinoma tumor formation by inhibiting angiogenesis. Cancer Res. 70, 5567–5576. 10.1158/0008-5472.CAN-09-4510. [PubMed: 20551050]

Lou N, Takano T, Pei Y, Xavier AL, Goldman SA, Nedergaard M, 2016. Purinergic receptor P2RY12-dependent microglial closure of the injured blood-brain barrier. Proc. Natl. Acad. Sci. USA 113, 1074–1079. 10.1073/pnas.1520398113. [PubMed: 26755608]

Luo W, Lin GN, Song W, Zhang Y, Lai H, Zhang M, Miao J, Cheng X, Wang Y, Li W, Wei W, Gao W-Q, Yang R, Wang J, 2021. Single-cell spatial transcriptomic analysis reveals common and divergent features of developing postnatal granule cerebellar cells and medulloblastoma. BMC Biol. 19, 135. 10.1186/s12915-021-01071-8. [PubMed: 34210306]

Luo J, Rasmussen IJ, Nordestgaard BG, Tybjærg-Hansen A, Thomassen JQ, Frikke-Schmidt R, 2025. Cardiovascular diseases and risk of dementia in the general population. Eur. J. Prev. Cardiol 10.1093/eurjpc/zwaf129zwaf129.

Lyons A, Lynch AM, Downer EJ, Hanley R, O'Sullivan JB, Smith A, Lynch MA, 2009. Fractalkine-induced activation of the phosphatidylinositol-3 kinase pathway attentuates microglial activation in vivo and in vitro. J. Neurochem 110, 1547–1556. 10.1111/j.1471-4159.2009.06253.x. [PubMed: 19627440]

Mathys H, Davila-Velderrain J, Peng Z, Gao F, Mohammadi S, Young JZ, Menon M, He L, Abdurrob F, Jiang X, Martorell AJ, Ransohoff RM, Hafler BP, Bennett DA, Kellis M, Tsai L-H, 2019. Single-cell transcriptomic analysis of Alzheimer's disease. Nature 570, 332–337. 10.1038/s41586-019-1195-2. [PubMed: 31042697]

Mathys H, Boix CA, Akay LA, Xia Z, Davila-Velderrain J, Ng AP, Jiang X, Abdelhady G, Galani K, Mantero J, Band N, James BT, Babu S, Galiana-Melendez F, Louderback K, Prokopenko D, Tanzi RE, Bennett DA, Tsai L-H, Kellis M, 2024. Single-cell multiregion dissection of Alzheimer's disease. Nature 632, 858–868. 10.1038/s41586-024-07606-7. [PubMed: 39048816]

Mildner A, Huang H, Radke J, Stenzel W, Priller J, 2017. P2Y12 receptor is expressed on human microglia under physiological conditions throughout development and is sensitive to neuroinflammatory diseases. Glia 65, 375–387. 10.1002/glia.23097. [PubMed: 27862351]

Mitroi DN, Tian M, Kawaguchi R, Lowry WE, Carmichael ST, 2022. Single-nucleus transcriptome analysis reveals disease- and regeneration-associated endothelial cells in white matter vascular dementia. J. Cell. Mol. Med 26, 3183–3195. 10.1111/jcmm.17315. [PubMed: 35543222]

Morabito S, Miyoshi E, Michael N, Shahin S, Martini AC, Head E, Silva J, Leavey K, Perez-Rosendahl M, Swarup V, 2021. Single-nucleus chromatin accessibility and transcriptomic characterization of Alzheimer's disease. Nat. Genet 53, 1143–1155. 10.1038/s41588-021-00894-z. [PubMed: 34239132]

Neary D, Snowden JS, Gustafson L, Passant U, Stuss D, Black S, Freedman M, Kertesz A, Robert PH, Albert M, Boone K, Miller BL, Cummings J, Benson DF, 1998. Frontotemporal lobar degeneration: a consensus on clinical diagnostic criteria. Neurology 51, 1546–1554. 10.1212/wnl.51.6.1546. [PubMed: 9855500]

Neufeld G, Sabag AD, Rabinovicz N, Kessler O, 2012. Semaphorins in angiogenesis and tumor progression. Cold Spring Harb. Perspect. Med 2, a006718. 10.1101/cshperspect.a006718. [PubMed: 22315716]

Newell KL, Hyman BT, Growdon JH, Hedley-Whyte ET, 1999. Application of the National Institute on Aging (NIA)-Reagan institute criteria for the neuropathological diagnosis of Alzheimer disease. J. Neuropathol. Exp. Neurol 58, 1147–1155. 10.1097/00005072-199911000-00004. [PubMed: 10560657]

Nordengen K, Kirsebom B-E, Henjum K, Selnes P, Gísladóttir B, Wettergreen M, Torsetnes SB, Grøntvedt GR, Waterloo KK, Aarsland D, Nilsson LNG, Fladby T 2019., Glial activation and inflammation along the Alzheimer's disease continuum. J. Neuroinflammation 16, 46. 10.1186/s12974-019-1399-2. [PubMed: 30791945]

Olah M, Menon V, Habib N, Taga MF, Ma Y, Yung CJ, Cimpean M, Khairallah A, Coronas-Samano G, Sankowski R, Grün D, Kroshilina AA, Dionne D, Sarkis RA, Cosgrove GR, Helgager J, Golden JA, Pennell PB, Prinz M, Vonsattel JPG, Teich AF, Schneider JA, Bennett DA, Regev

A, Elyaman W, Bradshaw EM, De Jager PL, 2020. Single cell RNA sequencing of human microglia uncovers a subset associated with Alzheimer's disease. Nat. Commun 11, 6129. 10.1038/s41467-020-19737-2. [PubMed: 33257666]

Reimand J, Kull M, Peterson H, Hansen J, Vilo J, 2007. G:profiler—a web-based toolset for functional profiling of gene lists from large-scale experiments. Nucleic Acids Res. 35, W193–W200. 10.1093/nar/gkm226. [PubMed: 17478515]

Reine TM, Vuong TT, Rutkovskiy A, Meen AJ, Vaage J, Jenssen TG, Kolset SO, 2015. Serglycin in quiescent and proliferating primary endothelial cells. PLoS One 10, e0145584. 10.1371/journal.pone.0145584. [PubMed: 26694746]

Robinson MD, McCarthy DJ, Smyth GK, 2010. edgeR: a Bioconductor package for differential expression analysis of digital gene expression data. Bioinformatics 26, 139–140. 10.1093/bioinformatics/btp616. [PubMed: 19910308]

Sakurai A, Doçi CL, Gutkind JS, 2012. Semaphorin signaling in angiogenesis, lymphangiogenesis and cancer. Cell Res. 22, 23–32. 10.1038/cr.2011.198. [PubMed: 22157652]

Schuff N, Matsumoto S, Kmiecik J, Studholme C, Du A, Ezekiel F, Miller BL, Kramer JH, Jagust WJ, Chui HC, Weiner MW, 2009. Cerebral blood flow in ischemic vascular dementia and Alzheimer's disease, measured by arterial spinlabeling magnetic resonance imaging. Alzheimers Dement. J. Alzheimers Assoc 5, 454–462. 10.1016/j.jalz.2009.04.1233.

Song WM, Joshita S, Zhou Y, Ulland TK, Gilfillan S, Colonna M, 2018. Humanized TREM2 mice reveal microglia-intrinsic and -extrinsic effects of R47H polymorphism. J. Exp. Med 215, 745–760. 10.1084/jem.20171529. [PubMed: 29321225]

Song R, Pan K-Y, Xu H, Qi X, Buchman AS, Bennett DA, Xu W, 2021. Association of cardiovascular risk burden with risk of dementia and brain pathologies: a population-based cohort study. Alzheimers Dement. 17, 1914–1922. 10.1002/alz.12343. [PubMed: 34310004]

Souma T, Thomson BR, Heinen S, Anna Carota I, Yamaguchi S, Onay T, Liu P, Ghosh AK, Li C, Eremina V, Hong Y-K, Economides AN, Vestweber D, Peters KG, Jin J, Quaggin SE, 2018. Context-dependent functions of angiopoietin 2 are determined by the endothelial phosphatase VEPTP. Proc. Natl. Acad. Sci 115, 1298–1303. 10.1073/pnas.1714446115. [PubMed: 29358379]

Spangenberg EE, Green KN, 2017. Inflammation in Alzheimer's disease: lessons learned from microglia-depletion models. Brain Behav. Immun 61, 1–11. 10.1016/j.bbi.2016.07.003. [PubMed: 27395435]

STAR: Ultrafast Universal RNA-Seq Aligner, 2025. PMC [WWW Document]. URL. https://www.ncbi.nlm.nih.gov/pmc/articles/PMC3530905/ (accessed 6.1.23).

Stritt S, Nurden P, Nurden AT, Schved J-F, Bordet J-C, Roux M, Alessi M-C, Trégouët D-A, Mäkinen T, Giansily-Blaizot M, 2023. APOLD1 loss causes endothelial dysfunction involving cell junctions, cytoskeletal architecture, and Weibel-Palade bodies, while disrupting hemostasis. Haematologica 108, 772–784. 10.3324/haematol.2022.280816. [PubMed: 35638551]

Tanaka I, Dayde D, Tai MC, Mori H, Solis LM, Tripathi SC, Fahrmann JF, Unver N, Parhy G, Jain R, Parra ER, Murakami Y, Aguilar-Bonavides C, Mino B, Celiktas M, Dhillon D, Casabar JP, Nakatochi M, Stingo F, Baladandayuthapani V, Wang H, Katayama H, Dennison JB, Lorenzi PL, Do K-A, Fujimoto J, Behrens C, Ostrin EJ, Rodriguez-Canales J, Hase T, Fukui T, Kajino T, Kato S, Yatabe Y, Hosoda W, Kawaguchi K, Yokoi K, Chen-Yoshikawa TF, Hasegawa Y, Gazdar AF, Wistuba II, Hanash S, Taguchi A, 2022. SRGN-triggered aggressive and immunosuppressive phenotype in a subset of TTF-1-negative lung adenocarcinomas. J. Natl. Cancer Inst 114, 290–301. 10.1093/jnci/djab183. [PubMed: 34524427]

Tayler H, Miners JS, Güzel Ö, MacLachlan R, Love S, 2021. Mediators of cerebral hypoperfusion and blood-brain barrier leakiness in Alzheimer's disease, vascular dementia and mixed dementia. Brain Pathol. Zurich Switz 31, e12935. 10.1111/bpa.12935.

Thrupp N, Sala Frigerio C, Wolfs L, Skene NG, Fattorelli N, Poovathingal S, Fourne Y, Matthews PM, Theys T, Mancuso R, de Strooper B, Fiers M, 2020. Single-nucleus RNA-Seq is not suitable for detection of microglial activation genes in humans. Cell Rep. 32, 108189. 10.1016/j.celrep.2020.108189. [PubMed: 32997994]

Toda T, Parylak S, Linker SB, Gage FH, 2019. The role of adult hippocampal neurogenesis in brain health and disease. Mol. Psychiatry 24, 67–87. 10.1038/s41380-018-0036-2. [PubMed: 29679070]

Uddin Md.S., Lim LW, 2022. Glial cells in Alzheimer's disease: from neuropathological changes to therapeutic implications. Ageing Res. Rev 78, 101622. 10.1016/j.arr.2022.101622. [PubMed: 35427810]

Ueno M, Chiba Y, Matsumoto K, Murakami R, Fujihara R, Kawauchi M, Miyanaka H, Nakagawa T, 2016. Blood-brain barrier damage in vascular dementia. Neuropathol. Off. J. Jpn. Soc. Neuropathol 36, 115–124. 10.1111/neup.12262.

Vågesjö E, Parv K, Ahl D, Seignez C, Herrera Hidalgo C, Giraud A, Leite C, Korsgren O, Wallén H, Juusola G, Hakovirta HH, Rundqvist H, Essand M, Holm L, Johnson RS, Thålin C, Korpisalo P, Christoffersson G, Phillipson M, 2021. Perivascular macrophages regulate blood flow following tissue damage. Circ. Res 128, 1694–1707. 10.1161/CIRCRESAHA.120.318380. [PubMed: 33878889]

Vestweber D, 2021. Vascular endothelial protein tyrosine phosphatase regulates endothelial function. Physiol. Bethesda Md 36, 84–93. 10.1152/physiol.00026.2020.

Wang H, 2021. Microglia heterogeneity in Alzheimer's disease: insights from single-cell technologies. Front. Synaptic Neurosci 13, 773590. 10.3389/fnsyn.2021.773590. [PubMed: 35002670]

Wightman DP, Jansen IE, Savage JE, Shadrin AA, Bahrami S, Holland D, Rongve A, Børte S, Winsvold BS, Drange OK, Martinsen AE, Skogholt AH, Willer C, Bråthen G, Bosnes I, Nielsen JB, Fritsche LG, Thomas LF, Pedersen LM, Gabrielsen ME, Johnsen MB, Meisingset TW, Zhou W, Proitsi P, Hodges A, Dobson R, Velayudhan L, Heilbron K, Auton A, Sealock JM, Davis LK, Pedersen NL, Reynolds CA, Karlsson IK, Magnusson S, Stefansson H, Thordardottir S, Jonsson PV, Snaedal J, Zettergren A, Skoog I, Kern S, Waern M, Zetterberg H, Blennow K, Stordal E, Hveem K, Zwart J-A, Athanasiu L, Selnes P, Saltvedt I, Sando SB, Ulstein I, Djurovic S, Fladby T, Aarsland D, Selbæk G, Ripke S, Stefansson K, Andreassen OA, Posthuma D, 2021. A genome-wide association study with 1,126,563 individuals identifies new risk loci for Alzheimer's disease. Nat. Genet 53, 1276–1282. 10.1038/s41588-021-00921-z. [PubMed: 34493870]

Wolf Y, Yona S, Kim K-W, Jung S, 2013. Microglia, seen from the CX3CR1 angle. Front. Cell. Neurosci 7.

Wolters FJ, Zonneveld HI, Hofman A, van der Lugt A, Koudstaal PJ, Vernooij MW, Ikram MA, 2017. Cerebral perfusion and the risk of dementia. Circulation. 10.1161/CIRCULATIONAHA.117.027448.

Wu H, Kirita Y, Donnelly EL, Humphreys BD, 2019. Advantages of single-nucleus over single-cell RNA sequencing of adult kidney: rare cell types and novel cell states revealed in fibrosis. J. Am. Soc. Nephrol. JASN 30, 23–32. 10.1681/ASN.2018090912. [PubMed: 30510133]

Yan D, Cui D, Zhu Y, Chan CKW, Choi CHJ, Liu T, Tsao SW, Ma S, Cheung ALM, 2022. Serglycin-induced interleukin-1β from oesophageal cancer cells upregulate hepatocyte growth factor in fibroblasts to promote tumour angiogenesis and growth. Clin. Transl. Med 12, e1031. 10.1002/ctm2.1031. [PubMed: 35994394]

Yang S, Corbett SE, Koga Y, Wang Z, Johnson WE, Yajima M, Campbell JD, 2020. Decontamination of ambient RNA in single-cell RNA-seq with DecontX. Genome Biol. 21, 57. 10.1186/s13059-020-1950-6. [PubMed: 32138770]

Yang AC, Vest RT, Kern F, Lee DP, Agam M, Maat CA, Losada PM, Chen MB, Schaum N, Khoury N, Toland A, Calcuttawala K, Shin H, Pálovics R, Shin A, Wang EY, Luo J, Gate D, Schulz-Schaeffer WJ, Chu P, Siegenthaler JA, McNerney MW, Keller A, Wyss-Coray T, 2022. A human brain vascular atlas reveals diverse mediators of Alzheimer's risk. Nature 603, 885–892. 10.1038/s41586-021-04369-3. [PubMed: 35165441]

Zhou Y, Song WM, Andhey PS, Swain A, Levy T, Miller KR, Poliani PL, Cominelli M, Grover S, Gilfillan S, Cella M, Ulland TK, Zaitsev K, Miyashita A, Ikeuchi T, Sainouchi M, Kakita A, Bennett DA, Schneider JA, Nichols MR, Beausoleil SA, Ulrich JD, Holtzman DM, Artyomov MN, Colonna M, 2020. Human and mouse single-nucleus transcriptomics reveal TREM2-dependent and TREM2-independent cellular responses in Alzheimer's disease. Nat. Med 26, 131–142. 10.1038/s41591-019-0695-9. [PubMed: 31932797]

Zujovic V, Benavides J, Vigé X, Carter C, Taupin V, 2000. Fractalkine modulates TNF-alpha secretion and neurotoxicity induced by microglial activation. Glia 29, 305–315. [PubMed: 10652441]

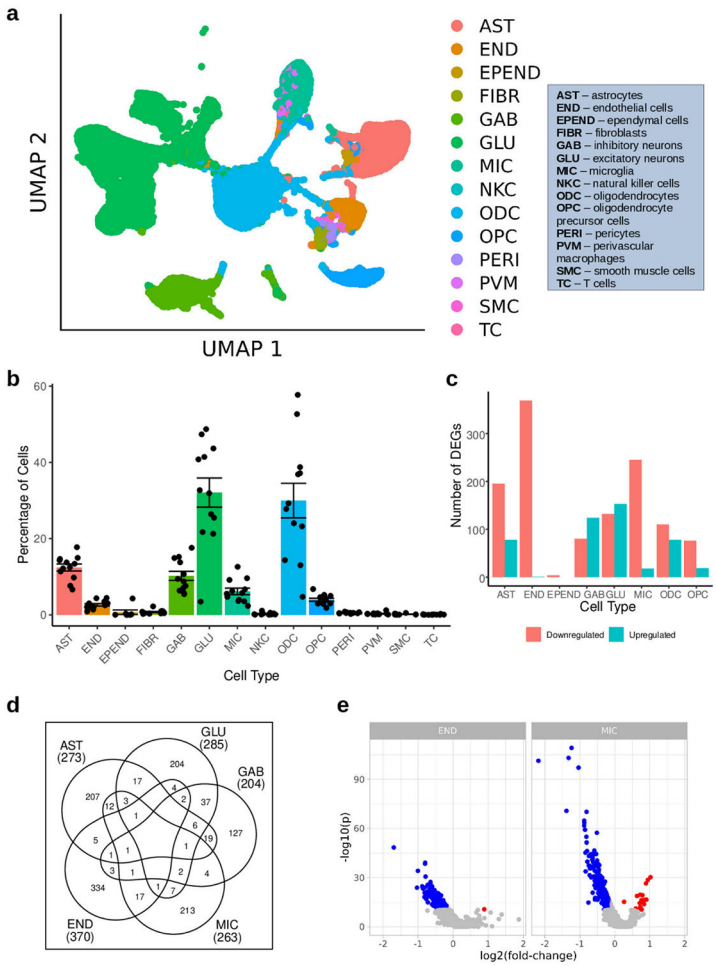

Fig. 1. Differentially expressed genes across cell types.

a) UMAP plots showing the distribution of cell types in the dataset (n = 12 samples). b) Bar plot showing mean individual percentage of each cell type with ±1 standard error bar and individual sample percentages overlaid (n = 12 samples). c) Number of up- and downregulated (in AD+Vas relative to other AD samples) differentially expressed genes (DEGs) by cell type. Cell types with very few DEGs were excluded. d) Venn diagram showing DEG overlap in the top 5 cell types by number of DEGs. Total number of DEGs is indicated in parentheses. e) Volcano plot for microglia and endothelial cells with DEGs highlighted in blue and red.

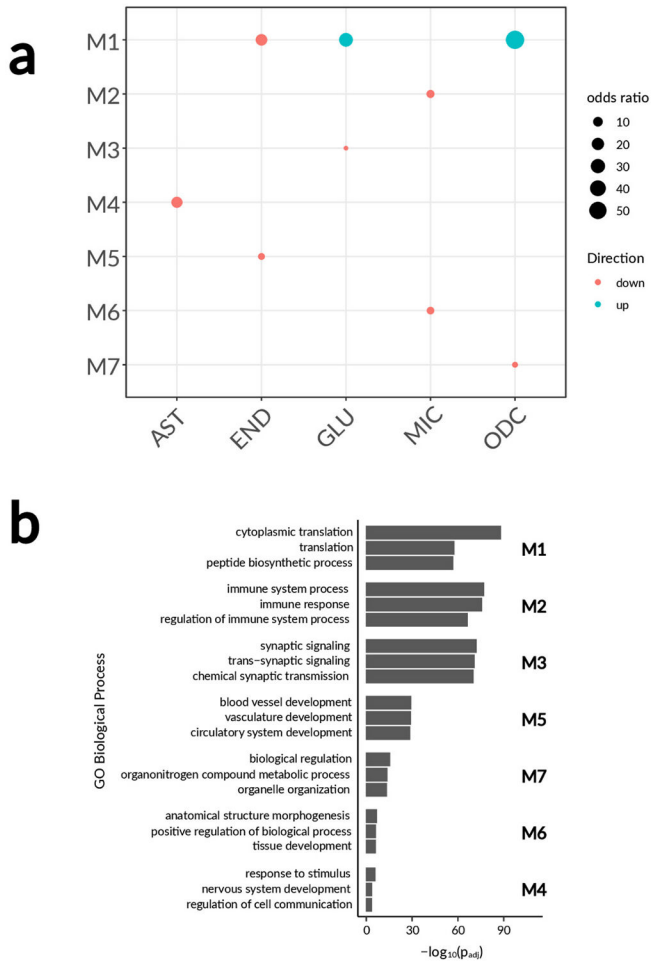

Fig. 2. Co-expression module enrichment reveals cell type-specific patterns.

a) Plot showing the enrichment by cell type and colored by enrichment status in up- or downregulated differentially expressed genes (DEGs) in significant modules-cell type pairs ($p_{FDR} < 0.01$). Modules are enriched in the upregulated or downregulated DEGs of astrocytes (AST), endothelial cells (END), oligodendrocytes (ODC), excitatory neurons (GLU), and microglia (MIC). The size of each dot is a function of Fisher's exact test odds ratios for the DEGs being a member of each respective module. b) Three most significant Gene Ontology (GO) Biological Process results for each module.

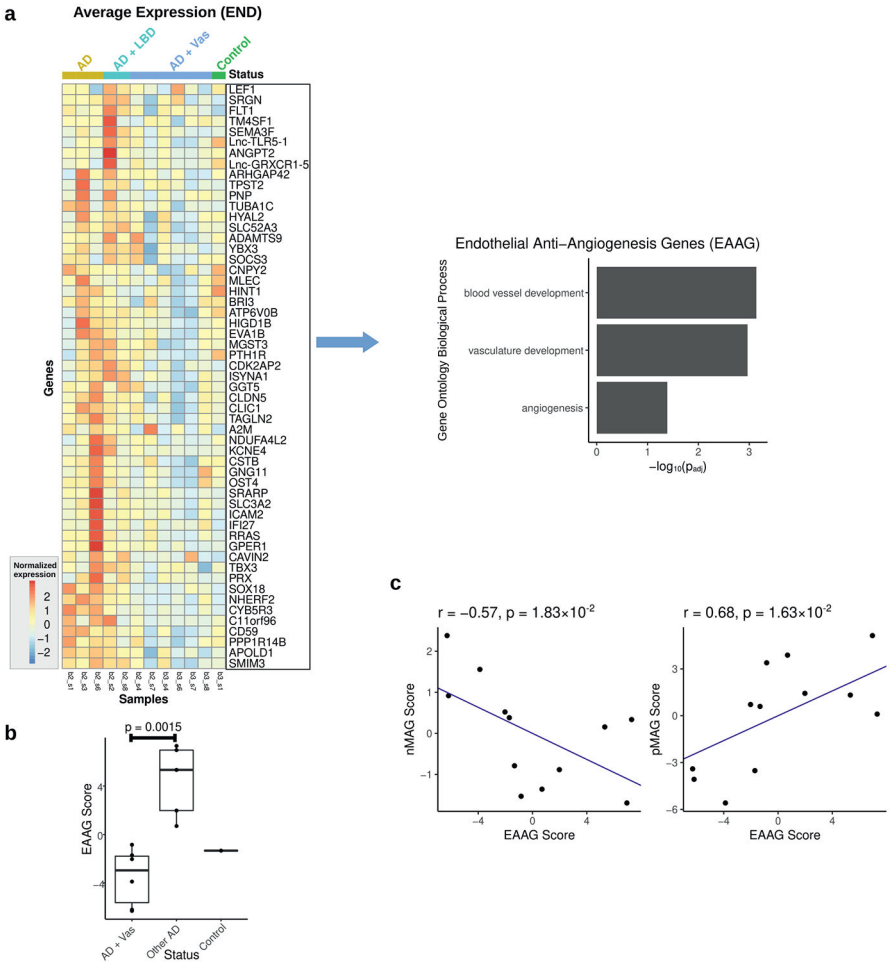

Fig. 3. Endothelial anti-angiogenesis genes are downregulated in AD + Vas and associated with microglia activation.

a) Left portion of the panel is a heatmap of average normalized expression values showing the downregulation of endothelial anti-angiogenesis. Genes (EAAG) in samples from subjects with AD+Vas compared to other AD subjects. The singular control sample was included in the heatmap. Right portion of the panel shows the Gene Ontology (GO) Biological Process terms enriched in the EAAGs sorted by enrichment p_{FDR}. b) Boxplot showing the downregulation of the aggregated EAAG score in subjects with AD+Vas (n = 6) compared to other AD subjects (n = 5) and one control subject. c) Scatter plots showing correlations of EAAG score with negative (nMAG) and positive (pMAG) microglial activation gene scores.

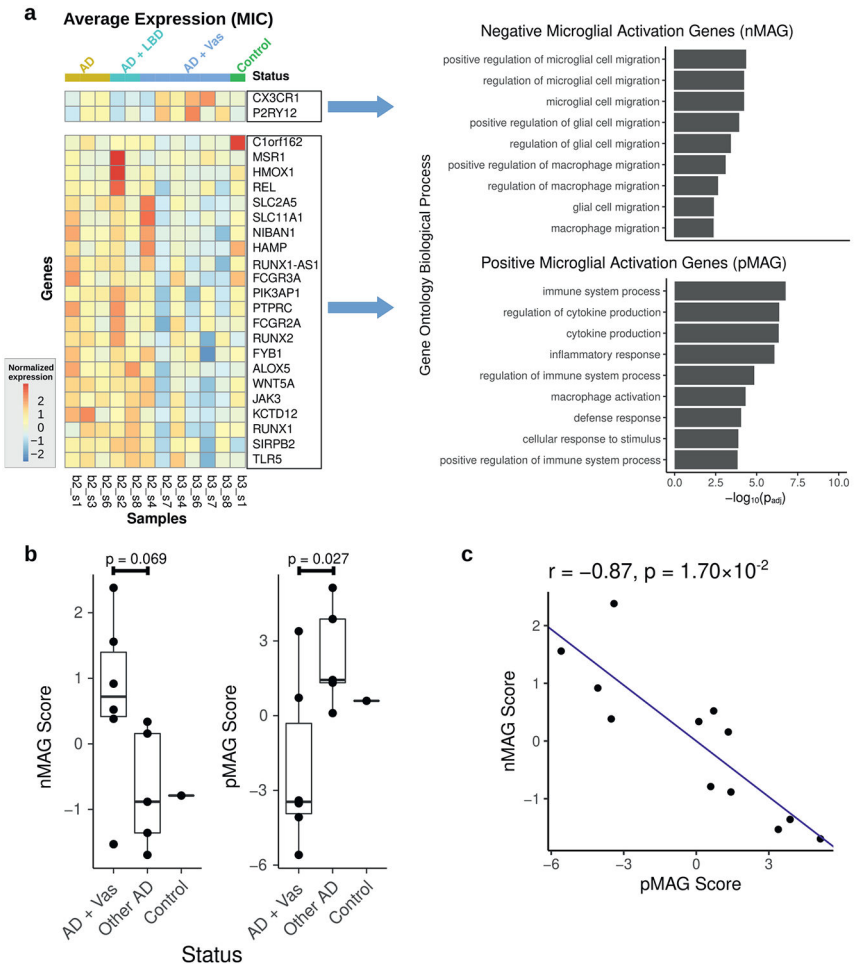

Fig. 4. Microglial activation program is downregulated in AD + Vas.

a) Heatmap of average normalized negative (nMAG) and positive (pMAG) microglial activation gene scores showing the downregulation of pMAGs and the upregulation of nMAGs in samples from subjects with AD+Vas ($n = 6$) compared to other AD subjects ($n = 5$) and one control. Enriched Gene Ontology (GO) Biological Process terms for each of the two gene sets can be found to the right, with each sorted by enrichment p_{FDR}. b) Boxplot showing distribution of aggregated nMAG and pMAG scores in subjects according to AD diagnosis. c) Scatter plot showing the negative correlation between nMAG and pMAG scores.

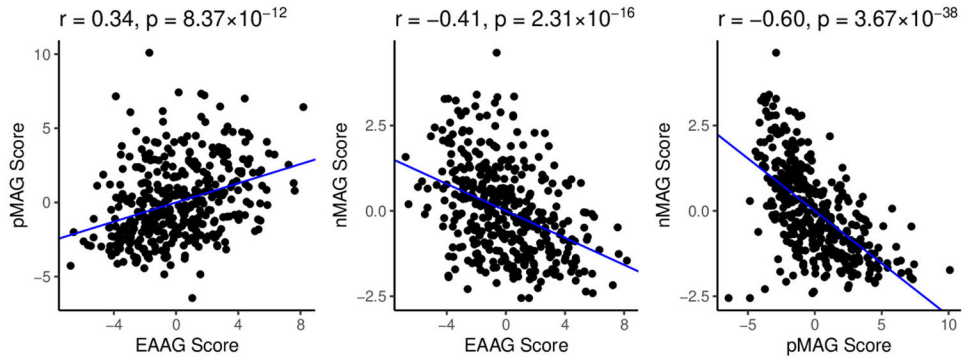

Fig. 5. Correlation of microglial activation and endothelial anti-angiogenesis genes in the ROSMAP dataset.

The correlation patterns among negative microglial activation (nMAG), positive microglial activation (pMAG), and endothelial anti-angiogenesis gene (EAAG) scores derived from snRNAseq data generated from the dorsolateral prefrontal cortex of 393 ROSMAP individuals are the same as those generated from the hippocampus for the BU-ADRC individuals.

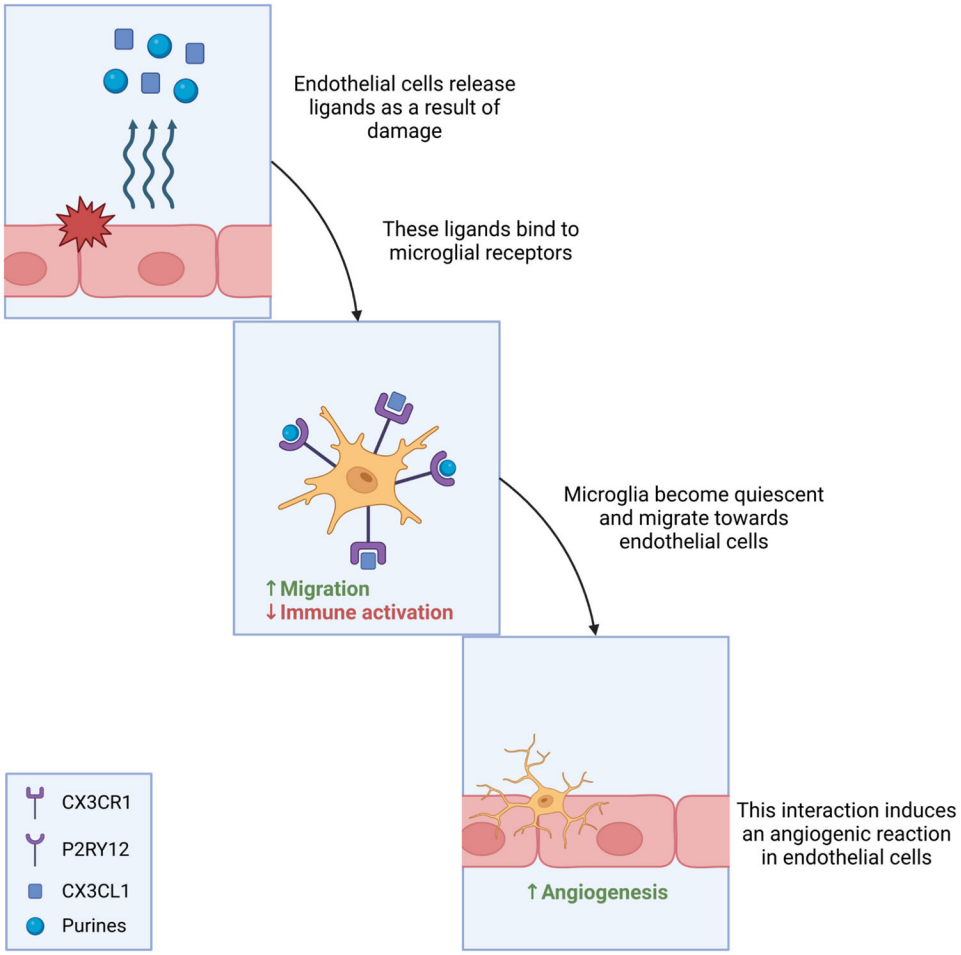

Fig. 6. Microglia-endothelial cell interaction.

We propose that the upregulation of nMAGs and downregulation of EAAGs is the result of damaged endothelial cells releasing *P2RY12* ligands, causing microglia to migrate to and induce an angiogenic reaction in them.

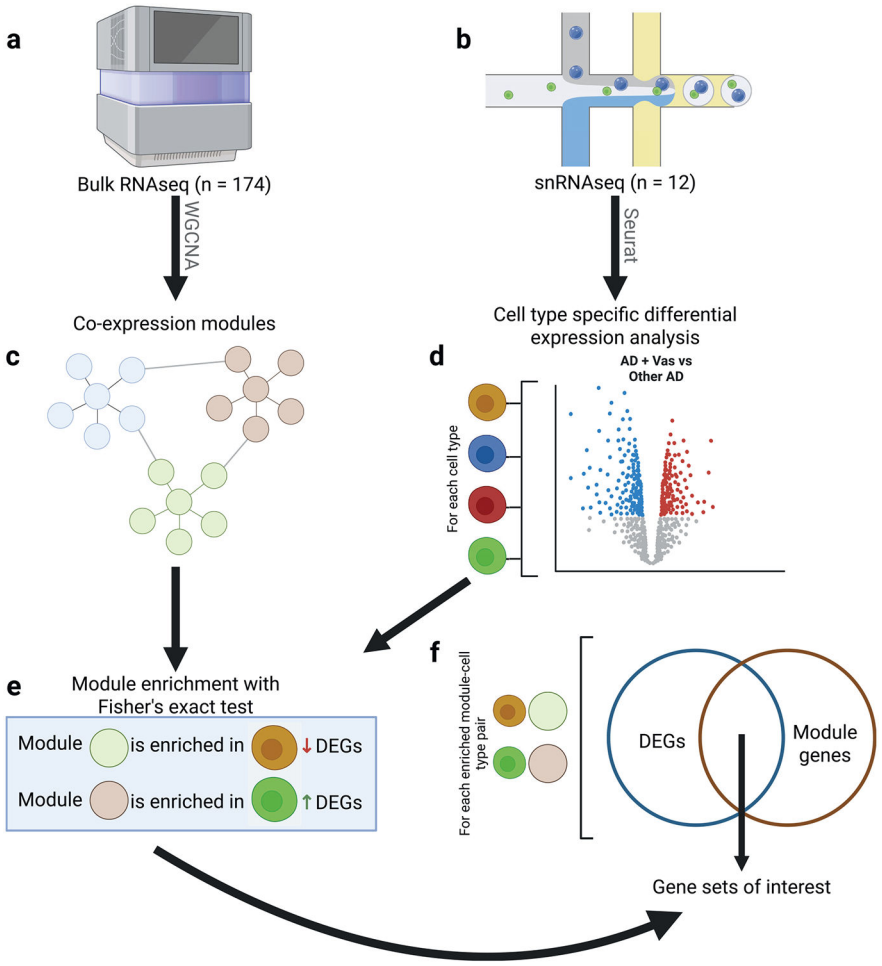

Fig. 7. Overview of methods.

a) Bulk and b) Single-nucleus RNA sequencing data were generated from hippocampal tissue obtained from pathologically-confirmed AD cases with or without co-existing pathologies and control individuals. c) Gene co-expression modules were generated from bulk RNAseq data using weighted gene co-expression network analysis (WGCNA). d) Gene expression in each cell type was compared between AD+Vas subjects and all other AD subjects using Seurat. e) WGCNA co-expression module genes and the cell type-level differentially expressed genes (DEGs) were used to prioritize modules based on enrichment. f) Gene sets were created from the overlap between DEGs for a cell type and their respective enriched module.

Table 1

Characteristics of subjects with snRNAseq data according to pathological diagnosis.

	AD alone	AD + LBD	AD + Vas	Control
N=12	3	2	6	1
Mean Age (range)	82.7 (79–86)	83.0 (79–87)	87.0 (84–89)	82.0
Male: Female Ratio	2:1	1:1	4:2	0:1
Mean Braak Stage (range)	5.0 (3–6)	4.0 (3–5)	4.8 (3–6)	2.0
Mean CERAD Score (range)	1.7 (1–3)	1.5 (1–2)	1.5 (1–3)	4.0

AD = Alzheimer disease; LBD = Lewy body disease; Vas = vascular disease.

Table 2

Demographic overview of BU-ADRC bulk RNAseq samples after filtering.

	AD	AD + LBD	AD + Vas	AD + Other	Control
N	73	43	54	4	17
Age (±sd)	77.0 (±8.48)	79.9 (±6.08)	84.0 (±9.35)	80.2 (±5.56)	89.0 (±9.77)
Male: Female Ratio	60:13	36:7	39:15	4:0	10:7
Braak Stage (±sd)	5.53 (±0.647)	5.28 (±0.854)	5.28 (±0.856)	4.25 (±0.500)	2.29 (±0.985)
CERAD Score (±sd)	1.14 (±0.419)	1.19 (±0.394)	1.22 (±0.538)	1.25 (±0.500)	3.12 (±0.993)

AD = Alzheimer disease; LBD = Lewy body disease; Vas = vascular disease; sd = standard deviation.

Table 3

Top-ranked gene co-expression modules.

Module*	Odds Ratio	p-value	p_{FDR}	Direction	Cell Type
M4	1.52×10^{1}	6.71×10^{-22}	6.76×10^{-19}	Down	AST
M5	3.91×10^{0}	4.40×10^{-15}	4.43×10^{-12}	Down	END
M1	5.88×10^{1}	3.25×10^{-14}	3.27×10^{-11}	Up	ODC
M1	1.72×10^{1}	3.60×10^{-12}	3.62×10^{-9}	Down	END
M1	2.79×10^{1}	3.11×10^{-11}	3.13×10^{-8}	Up	GLU
M2	5.99×10^{0}	2.91×10^{-10}	2.92×10^{-7}	Down	MIC
M7	2.85×10^{0}	2.79×10^{-7}	2.80×10^{-4}	Down	ODC
M3	2.44×10^{0}	3.87×10^{-7}	3.88×10^{-4}	Down	GLU
M6	5.20×10^{0}	9.87×10^{-6}	9.87×10^{-3}	Down	MIC

AST = astrocytes; END = endothelial cells; ODC = oligodendrocytes; GLU = excitatory neurons; MIC = microglia.

*Includes co-expression modules which are significantly ($p_{FDR} < 0.01$) enriched for differentially expressed genes, either upregulated or downregulated.